

Geological Society, London, Special Publications

## **Metamorphic evolution of a very low- to low-grade metamorphic core complex (Danubian window) in the South Carpathians**

Magda Ciulavu, Rafael Ferreiro Mählmann, Stefan M. Schmid, Heiko Hofmann, Antoneta Seghedi and Martin Frey

*Geological Society, London, Special Publications* 2008; v. 298; p. 281-315  
doi:10.1144/SP298.14

---

**Email alerting service**      [click here](#) to receive free email alerts when new articles cite this article

**Permission request**      [click here](#) to seek permission to re-use all or part of this article

**Subscribe**      [click here](#) to subscribe to Geological Society, London, Special Publications or the Lyell Collection

---

### **Notes**

**Downloaded by**      on 20 July 2008

---

# Metamorphic evolution of a very low- to low-grade metamorphic core complex (Danubian window) in the South Carpathians

MAGDA CIULAVU<sup>1,2,\*</sup>, RAFAEL FERREIRO MÄHLMANN<sup>1,3,§</sup>, STEFAN M. SCHMID<sup>4</sup>,  
HEIKO HOFMANN<sup>3</sup>, ANTONETA SEGHEDI<sup>2</sup> & MARTIN FREY<sup>1,†</sup>

<sup>1</sup>*Mineralogisch-Petrographisches Institut, Universität Basel, Bernoullistrasse 30,  
CH-4056 Basel, Switzerland*

<sup>2</sup>*Institutul Geologic al Romaniei, 1 Caransebes Street, RO 78 344 Bucharest 32, Romania*

<sup>3</sup>*Institut für Angewandte Geowissenschaften, TU Darmstadt, Schnittspahnstraße 9,  
D 64287 Darmstadt, Germany*

<sup>4</sup>*Geologisch-Paläontologisches Institut, Universität Basel, Bernoullistrasse 32,  
CH-4056 Basel, Switzerland*

*\*Now at Canadian Natural Resources Ltd., Calgary, Alberta, Canada*

*†Martin Frey died in a mountain accident during fieldwork in the Alps in September 2000.  
We thank him for stimulating our research on low-grade metamorphism.*

*§Current address: Darmstadt University of Technology, Faculty of Material und Geosciences,  
Institute of Applied Geosciences, Technical Petrology, Schnittspahnstraße 9, D-64287  
Darmstadt, Germany (e-mail: ferreiro@geo.tu-darmstadt.de)*

**Abstract:** The Danubian window, characterized by diagenetic to low greenschist facies conditions at a high thermal gradient, is evidently of great interest for methodological studies, because high metamorphic thermal gradient conditions during low grade metamorphism have received little attention so far. The general increase in metamorphic grade from SW to NE in the Danubian window is indicated by mineral Parageneses studies, as well as by illite Kübler index (KI) measurements and organic matter reflectance (OMR). For the first time, this study distinguishes between metamorphic conditions related to Jurassic ocean floor, Cretaceous nappe stacking, post-collisional accommodation and syn-kinematic Getic detachment metamorphism and cooling after Oligocene exhumation.

The occurrence of the prehnite–pumpellyite facies in the Severin–Cosustea units in the south-eastern area is the result of Cretaceous metamorphism. Remnants of ocean floor metamorphism prevailed. The highest pressure is constrained by the upper stability limit of prehnite to be at around 4.0 kbar. The Danubian units situated within the diagenetic zone were not below 200 °C, due to epidote formation. The KI, OMR and mineral data, indicate diagenetic conditions. Assuming temperatures between >200 and <250 °C, pressures between 1.8 and 2.6 kbar were calculated using kinetic and numerical maturity models.

Orogenic collisional Cretaceous peak pressure conditions of  $4.0 \pm 1.0$  kbar are found in the Danubian nappes not altered by a subsequent syn-detachment metamorphic overprint. Highest temperatures in chloritoid schists and epidote–hornblende-bearing mylonites have been inferred for samples from the northern border of the Danubian window (between >300 and <400 °C). Along a syn- to post-detachment retrograde pressure path, post-dating the chloritoid formation, the occurrence of clinozoisite + chlorite + quartz suggests temperatures >300 °C in the north-west, while the association andalusite + quartz and biotite + muscovite indicates temperatures between 370 and 400 °C at <3.5 kbar in the northeast.

It is demonstrated that the slope of the regression lines between KI and OMR data gives valuable qualitative information about the relative magnitudes of P and T: the slope of the regression line for the Danubian window samples indicates normal heat flow conditions during nappe stacking and hyperthermal conditions during the formation of the Getic detachment.

High thermal gradient conditions can easily be explained by partly isothermal decompression during the Getic detachment event, the elevation of the geotherm being caused by crustal thinning and rapid exhumation of the Danubian units. Probably, also a higher heat-flux prevailed at the end of the Getic detachment, at a time when the retrograde chloritoid decomposition reactions took place, documenting late-stage HT greenschist facies metamorphism.

## Location of the study area and geological Setting

The South Carpathians represent a roughly east–west-striking segment of the Carpathian loop, situated between the foredeep of the Getic depression in the south and the Transylvanian basin in the north (Fig. 1). Eastward, the mountain chain prolongates in the East Carpathian range in the bending area NE of Bucharest. Southwestward, they find their continuation in eastern Serbia and ultimately in the Balkanides of Bulgaria.

The South Carpathians consist of a pile of basement and cover nappes formed during Cretaceous orogeny (e.g. Săndulescu 1984, 1994). From bottom to top, this nappe stack comprises, the following units used as a reference to locate the metamorphic data of Figures 3 to 6: (1) a stack of Danubian thrust sheets (Upper and Lower Danubian nappes), consisting of pre-Mesozoic metamorphic and magmatic rocks (basement) and their Mesozoic cover; (2) due to a differing lithofacies compared to the other Danubian nappes, the Arjana cover nappe is shown, which occupies the structurally highest position within the Danubian nappe stack; (3) the Cosustea

mélange, mostly together with locally preserved tectonic slices of an ophiolitic-sedimentary sequence, representing remnants of the oceanic Severin nappe lithosphere (in Figs 2 and 3, both are shaded undifferentiated); and (4) the Getic and Supragetic nappes which mostly consist of Precambrian and Variscan basement, overlain by a Palaeozoic to Mesozoic cover.

The Severin Ocean opened during the Jurassic between the Danubian and Getic–Supragetic units, which were parts of the European Plate (Săndulescu 1975, 1994). Convergence in the Cretaceous led to the suturing (subduction and obduction) of the Severin oceanic lithosphere (Stănoiu 1972), followed by collision of the Severin and Getic–Supragetic units with the Danubian continental block during an orogenic stage in the Late Senonian. The final nappe stack was subsequently affected by orogen-parallel extension, which, according to fission-track data, led to final exhumation of the Danubian window during Eocene times (Schmid *et al.* 1998; Fügenschuh & Schmid 2005). The post-orogenic (i.e. post-Eocene) movements did not substantially alter the tectonic edifice as observed today, except for sinistral strike-slip motions in the order of 35 km along the Cerna–Jiu strike-slip fault (Berza & Drăgănescu 1988). The curved Cerna–Jiu fault (Fig. 2) can be

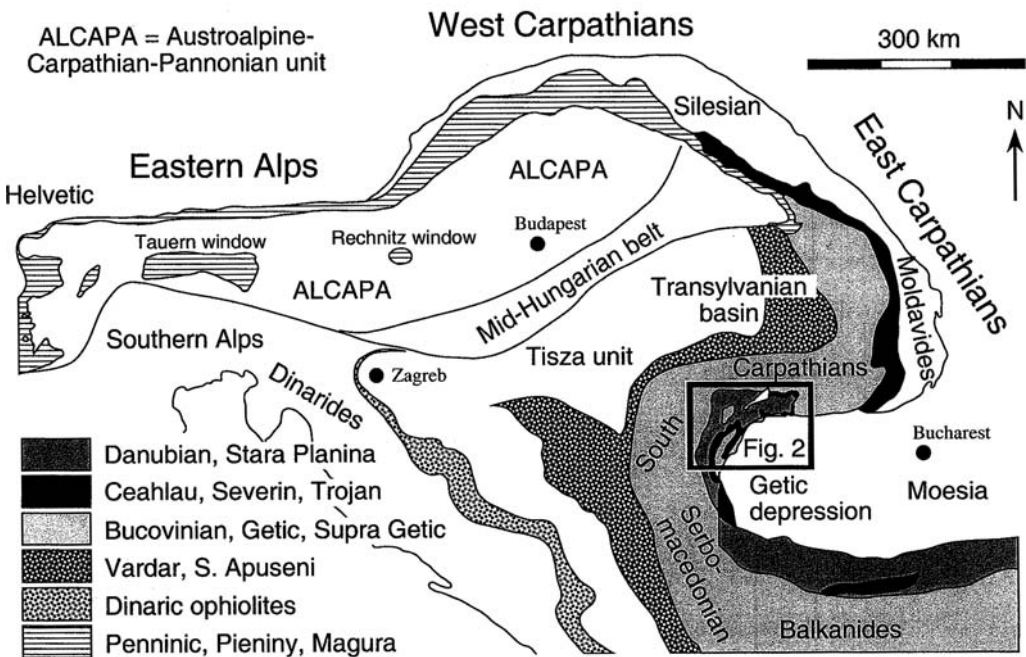
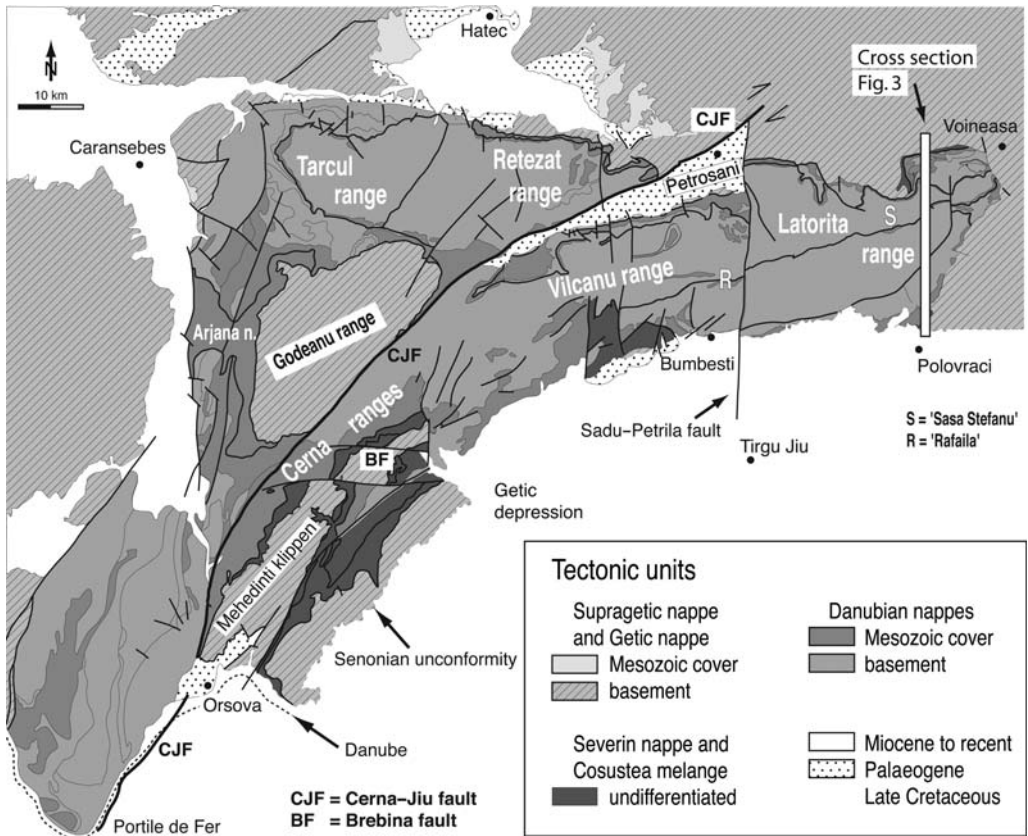


Fig. 1. Sketch map of the Alpine–Carpathian mountain chain and the main tectonic units (modified after Săndulescu 1994).



**Fig. 2.** Tectonic map of the Danubian window between Portile de Fer (Iron Gate) and the eastern end at Voineasa with the mountain ranges, localities and tectonic structures referred in the text (modified after Fügenschuh & Schmid 2005).

followed across the entire Danubian window, changing strike direction from NNE to SSW towards NE to SW following sub-parallel to the Carpathian bend. This strike-slip fault is directly related to the opening of the intramontane Petrosani basin, which formed during the Chattian to Badenian (Berza & Drăgănescu 1988; Ratschbacher *et al.* 1993). A south-directed thrusting onto the Getic depression (Fig. 2) occurred in the Miocene (Matenco *et al.* 1997).

Zircon fission-track data show that pervasive Cretaceous low-grade metamorphism (Alpine metamorphism) is restricted to the northern and northeastern part of the Danubian units and the Severin nappe. They are found below an extensional detachment (the Getic detachment), with the Getic and Supragetic units forming the non-metamorphic hanging wall (Schmid *et al.* 1998; Matenco & Schmid 1999; Fügenschuh & Schmid 2005). The Getic detachment is identical with the tectonic boundary between the Danubian–Severin nappes and the Getic–Supragetic units. Consequently, the studied area is restricted to the Danubian and Severin units.

The pioneering work of Mrazec (1898) and Murgoci (1905, 1912) indicated Alpine (Cretaceous) low-grade metamorphism in the Danubian units, based on the occurrence of chloritoid in Liassic sediments. This metamorphism was assumed to take place under anchimetamorphic to lowermost greenschist facies conditions (Savu 1970; Stănoiu *et al.* 1982), with a metamorphic grade increasing from southwest to northeast (Stănoiu *et al.* 1988). Part of the information available on this low-grade metamorphism in the northern and northeastern part of the window is also based on the occurrence of pyrophyllite (Paliuc 1972; Ianovici *et al.* 1981), kaolinite (thought to be Alpine) and chloritoid (Iancu *et al.* 1984; Iancu 1986). Alpine metamorphism was related to nappe thrusting by many authors (e.g. Manolescu 1937; Pop 1973; Berza *et al.* 1983).

Ocean-floor metamorphism was suggested in literature due to the studies of Savu *et al.* (1985) and Maruntiu (1987) for the mafic rocks of the Severin nappe, based on prehnite + pumpellyite  $\pm$  epidote  $\pm$  actinolite assemblages and K–Ar ages

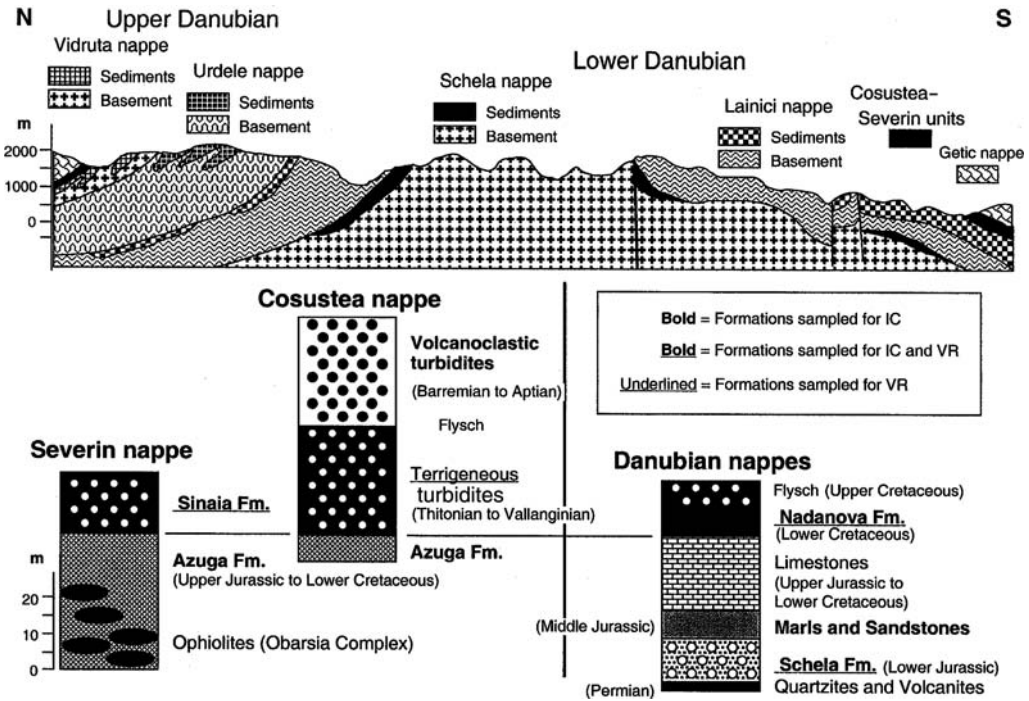


Fig. 3. Cross-section through the easternmost part of the Danubian window (for location see Fig. 2, strongly simplified after Schmid *et al.* 1998). Lithostratigraphic sections are compiled after Seghedi & Berza 1994). Flysch rocks in stratiform contact in Danubian nappes was not recognized during fieldwork, but often described in literature.

of the Jurassic/Cretaceous boundary (127 to 143 Ma according to Lemne *et al.* 1983). In the southwest, the regional occurrence of pumpellyite in successions derived from an accretionary complex and the local transition to pumpellyite-actinolite facies in the northeast were interpreted as evidence for subduction-related Alpine metamorphism of the Severin and Cosustea units (Seghedi *et al.* 1996; Ciulavu & Seghedi 1997). Petrological mineral data from literature need a more critical discussion corresponding to our present knowledge.

Recently, a series of papers used a combined structural and fission-track (FT) data approach in order to discuss the tectono-metamorphic evolution of the South Carpathians (e.g. Schmid *et al.* 1998; Bojar *et al.* 1998; Willingshofer 2000; Fügenschuh & Schmid 2005). Zircon and apatite fission-track ages from the Getic nappes indicate that the Getic nappes were not metamorphosed. Locally, the Getic basis and the Danubian nappes are generally characterized by Cretaceous ages. Cooling to near-surface temperatures of these units immediately followed Late Cretaceous orogeny. Eocene and Oligocene zircon and apatite ages from the part of the Danubian nappes situated SE of the

Cerna-Jiu fault monitor Late Palaeogene tectonic exhumation in the footwall of the Getic detachment, while zircon fission-track data from northwest of this fault indicate that slow cooling started during the Latest Cretaceous. The Danubian window is therefore a metamorphic core complex. The change from extension (Getic detachment) to strike-slip-dominated tectonics along the curved Cerna-Jiu fault allowed for further exhumation on the concave side of this strike-slip fault, while exhumation ceased on the convex side. The available FT data consistently indicate that the change to fast cooling associated with tectonic denudation by core complex formation did not occur before Late Eocene times, i.e. long after the cessation of Late Senonian thrusting. Core complex formation in the Danubian window is related to a larger-scale scenario that is characterized by the NNW-directed translation, followed by a 90° clockwise rotation of the Tisza-Dacia block due to rollback of the Carpathian embayment (Fügenschuh & Schmid 2005).

Based on a previous work (Ciulavu 2001), this paper represents a first systematic study attempting to map the grade of metamorphism in the Danubian window on Romanian territory.

Samples from Mesozoic units of the Danubian and Severin units have been analysed by optical microscopy, X-ray diffraction and electron-microprobe. Special attention has been paid to illite Kübler index, bituminite reflectance and vitrinite reflectance data because these methods proved to be efficient for the quantification of metamorphic grade under sub-greenschist facies conditions.

### Studied lithologies and sampling

The Danubian unit, subdivided due to lithofacies changes into Upper and Lower Danubian nappes (Berza *et al.* 1983, 1994, fig. 4), partly comprises Variscan basement nappes. The Variscan cycle ends with locally preserved Late Carboniferous molasse-like sediments and Permian red beds (Fig. 3) followed by Jurassic unconformity and syn-rift sediments. To study Alpine (Cretaceous) metamorphism, the work is focused on the post-Variscan cover.

Coal-bearing Liassic terrigenous deposits in Gresten facies (Schela Formation) directly overlie the basement or Permian rocks. In the western part of the Danubian window, this Schela Formation is overlain by Liassic black belemnite-bearing shales (Ohaba Beds), deposited under anoxic conditions (Năstăseanu 1979). These sediments and meta-sediments were sampled for all analytical methods used (Fig. 3).

The Middle Jurassic is represented by shallow marine quartzites or carbonate sandstones (Stănoiu 1973; Năstăseanu *et al.* 1985) in the central part of the Danubian window and by Bajocian limestones, Bathonian marls and Upper Jurassic nodular limestones 'ammonitico rosso' in the western part of the window (Codarcea & Raileanu 1960). Late Jurassic to Early Cretaceous carbonate platform sediments overlie these formations (Pop 1973; Berza *et al.* 1988a, b). Organic matter is very dispersed and mostly of inertinite and alginite composition not suitable for organic matter reflectance studies. Samples for clay mineral studies were collected.

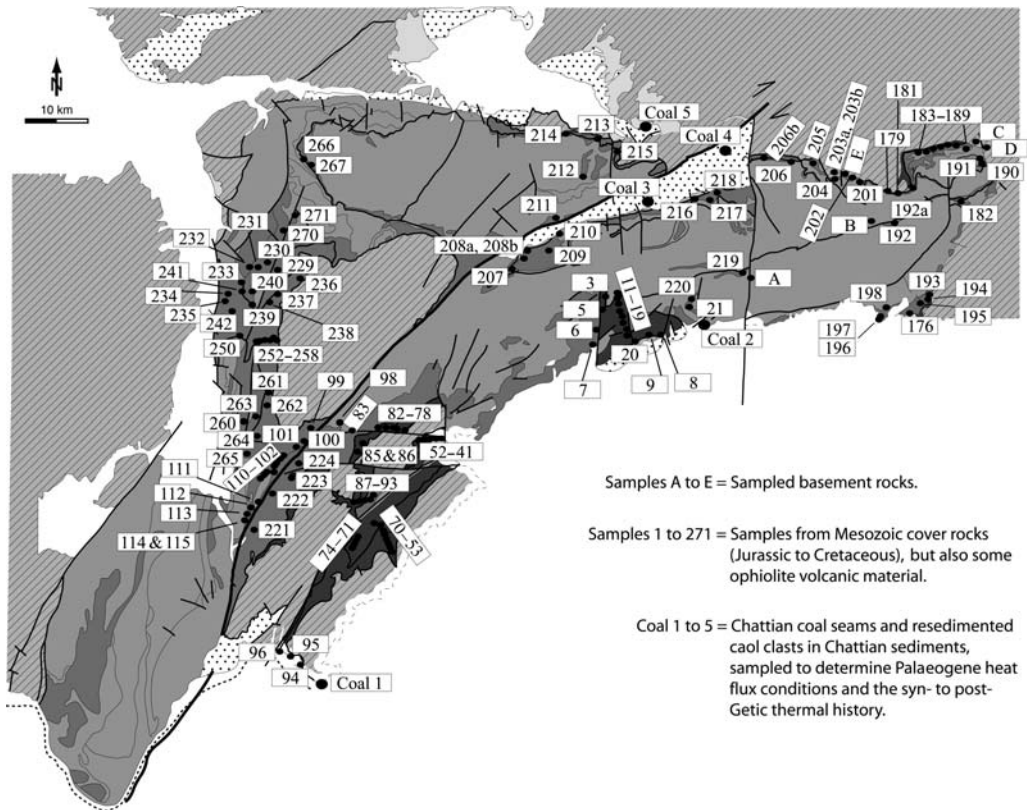


Fig. 4. Sample location map: data from Figs 5, 6, 7, 9, 11, 13 and 17 can be compared together and related to the corresponding location.

In the Arjana nappe west of the Godeanu range (Fig. 2), however, the Middle and Upper Jurassic succession is represented by volcano-sedimentary deposits with basic and alkaline lava flows (Russo-Săndulescu, pers. comm.), pyroclastic and epiclastic deposits, stromatactitic limestones and red shales (Codarcea 1940). The pelagic limestones and marls of the Nadvan Beds (Albian to Turonian age) and locally flysch sediments (Fig. 4) represent the youngest formations of the Danubian carbonate platform (e.g. Codarcea 1940; Pop 1973). In these lithological units, organic matter was locally observed but mostly altered by oxidation, as also the pelitic rocks and no authigenic mineral could be found mesoscopically. Sampling was very difficult.

Senonian 'wildflysch', represented by terrigenous and volcanoclastic turbidites (Fig. 4) with pelitic background sedimentation, forms the main compound of a tectonic mélange complex. The Cosustea mélange is shown undifferentiated with the Severin nappe in Figures 2, 3, 5, 7, 9 and 13. This mélange complex is characterized by a block-in-sheared matrix structure formed during early stages of tectonic accretion of these sediments to the overlying Severin and Getic units. Its contact to the underlying Nadvan Beds is always tectonic (Seghedi *et al.* 1996). Organic matter is very dispersed but sufficient and samples for clay mineral studies were collected. Sample locations are shown in Figure 4; the results shown on map Figures 5, 7, 9 and 13 can be related to these sample numbers and the numbers referred to in the text.

The Severin nappe overlies the accretionary wedge in some areas. It includes Late Jurassic radiolarian sediments (Azuga Beds) followed by Early Cretaceous terrigenous turbidites (Sinaia and Comarnic Flysch; see Codarcea 1940). The base of these sediments is formed by a strongly dismembered ophiolite mélange (Savu *et al.* 1985; Maruntiu 1987), consisting of ocean floor tholeiitic basalts (Cioflica *et al.* 1981), pillow basalts, gabbros and harzburgitic ultramafites.

The Getic–Supragetic nappes found above this accretionary wedge consist of a high-grade metamorphic Proterozoic basement (Iancu & Maruntiu 1994), locally covered by Late Carboniferous to Turonian sediments (a few samples were collected). They were already foliated during the Cretaceous but not overprinted by Alpine orogenic metamorphism. The contact at their base is deformed by the Getic detachment, which produced an extremely discrete jump in metamorphic grade between the non-metamorphic and brittle-deformed Getic–Supragetic nappes and the mylonitized greenschist to sub-greenschist facies units of the Danubian window (Schmid *et al.* 1998; Matenco & Schmid 1999).

## Analytical methods

### *Optical microscopy and electron-microprobe analysis*

Index mineral associations and facies-critical mineral parageneses in basalts, volcanics and volcanoclastics of the Severin and Cosustea nappes were investigated. In order to determine relationships between mineral growth and deformation, optical microscopy was combined with electron-microprobe analysis. For a better qualitative determination and quantification of metamorphic grade, the chemistry of the index minerals has been determined by electron-microprobe analysis (EMPA). Chlorite and white mica chemical compositions were used for approximate temperature and pressure estimates based on the methods of Cathelineau (1988) and Massonne & Schreyer (1987), respectively. Special interest has also been paid to a combined optical and electron-microprobe analysis of the pelitic rocks from the Schela formation in order to determine the lower stability limit of the chloritoid. The determination of chloritoid-formation reactions led to the mapping of a chloritoid-in isograd.

For chemical analyses, a Jeol JXA-8600 Superprobe with an accelerating voltage of 15 kV and a beam current of 10 nA was used. The data were reduced using the PROZA correction. The standards used are: olivine for Si and Mg, rutile for Ti, graphonite for Fe and Mn, orthoclase for K, albite for Na, wollastonite for Ca, gehlenite for Al and F-topaz for F.

### *X-ray powder diffraction (XRD)*

XRD analyses on pelitic lithologies were used to determine clay-mineral associations and the illite Kübler index (KI) on 170 samples from the Schela and Ohaba Formations, the Nadvan Beds, the Cosustea mélange, the Azuga Bed and Sinaia Flysch. The samples were crushed, decarbonated and prepared using the procedure described in detail by Schmidt *et al.* (1997).

All X-ray diffraction analyses were performed on a Bruker-AXS (Siemens) D-5000 diffractometer with the following settings: CuK $\alpha$ , 40 kV, 30 mA, V20-V20-2.0 mm slits, step size 0.02, counting time 2 seconds and rotation of the sample during measurement of run interval 2 to 50°2 $\theta$ . For samples with superposition of peaks in the 10 Å region, the interval 2 to 21°2 $\theta$  was remeasured with a 0.05° step size and 10 seconds counting time to obtain better diffractogram peak resolution. The clay mineral determination was assisted by Siemens software, namely 'Evaluation' and 'Profile fitting'. Mineral identification and profile

analyses were performed using the Siemens software 'Diffrac plus'.

The KI is defined as the full width at half maximum intensity (FWHM) of the first illite basal reflection. FWHM data obtained were transformed into KI values using the correlation from Frey (1986) in order to relate them to literature data with anchizone limits KI at 0.25 and  $0.42 \Delta^{\circ}2\theta$ . We used the KI calibration from the Frey standards. The conservative reason is that most papers on illite 'crystallinity' (the Kübler index was called illite 'crystallinity' (IC) in earlier publications) in the Alpine-Carpathian system refer to Frey (1986, 1987; for details see also Ferreiro Mählmann 1994).

### *Organic matter reflectance*

Organic matter reflectance has been determined on some samples used for the XRD study, for 31 samples from the Schela Formation, 5 from the Ohaba Formation, 4 from the Nadanova Beds and 8 from the Cosustea mélange, but also 3 from Chattian coal seams, and 2 from Chattian coaly clays. Mean random reflectance ( $R_r\%$ ) under non-polarized light of 546 nm wavelength was used for the Tertiary samples of the lignite to sub-bituminous stage A. Maximum reflectance ( $\%R_{\max}$ ) and minimum reflectance ( $\%R_{\min}$ ) have been measured on Jurassic and Cretaceous samples of the semi-anthracite to meta-anthracite stage (ASTM classification) using monochromatic polarized light (546 nm). Bireflectance ( $\%R_{\max} - \%R_{\min}$ ) has been used to distinguish the maceral group vitrinite and secondary maceral group bituminite (e.g. Stach *et al.* 1982; Robert 1988; Ferreiro Mählmann 2001).

The analyses were performed on a Leitz Orthoplan-photometer microscope with an ocular ( $\times 10$ ), an oil-immersion objective ( $\times 125$ ), and a photomultiplier with an aperture of  $2.5 \mu\text{m}^2$  using resin-mounted polished sections and applying standard methods (Robert 1988; Ferreiro Mählmann 1994, 2001).

## **Results**

### *Detrital mineral associations*

Samples from the pelitic background sedimentation of the Sinaia Flysch from the Azuga Bed, Cosustea mélange and Nadanova rocks only occasionally contain detrital mineral assemblages. Thin sections of the Schela and Ohaba Formations from the southern and central area of the Danubian window revealed clasts of white mica (phengite, muscovite-Ms), chlorite (Chl), zoned tourmaline (Tur), red allanite (All), rutile (Rt) and zircon (Zr).

In the central part there was also graphite (Gr) as mineral inclusion or determined by the polymodal highest reflecting organic matter population, light red garnet (Grt) and titanohematite (Ti-Hem) or hematite (Hem), sometimes together with very minor amounts of K-feldspar (Kfs), plagioclase (Plg), kyanite (Ky) and staurolite (St). All minerals are strongly rounded, and micas and graphite show kinking, disintegration and oxidation due to reworking. The detrital mineral assemblages are related to the basement rocks (also samples A and B) of the Variscan MP-MT metamorphic Dragsan Group (Berza & Seghedi 1983) and will be partly of interest regarding the educts of Cretaceous metamorphic mineral reactions.

### *Diagenetic and metamorphic mineral associations from the Danubian nappes*

EMPA data were used to verify optical studies of very small mineral phases and therefore chemical raw data are not presented in this study. A thermodynamic re-examination and geochemical investigation has to follow our petrogenetic determinations. Because also chemical chrochite-thermometry and phengite-barometry were only of informative character in the present paper, a chemical data presentation was thought to be of minor interest in the study.

Samples of Nadanova Beds consist of illite, chlorite, quartz and rare albite. In contrast, the Schela and Ohaba Formations often have a more complex modal composition and have additionally pyrophyllite, paragonite and chloritoid (Fig. 5).

*Kaolinite* (Kln) has been identified in some samples of the Schela Formation by XRD. Kaolinite was treated with dimethyl-sulphoxide (causing shift of the kaolinite (001) peak and, consequently, discriminating it from the chlorite (002) peak) or heated at  $550^{\circ}\text{C}$  (causing the breakdown of the kaolinite structure) and confirmed in a HRTEM study (D. Schmidt 'pers. comm.'). In the northeastern part of the Danubian window, *pyrophyllite* is frequently found in the Schela Formation (Al-rich schists).

*Illite-smectite mixed-layer clay minerals*, identified after a treatment with ethylene-glycol and heated to  $30^{\circ}\text{C}$  during 72 h, together with kaolinite and *corrensites* (in one sample), point to diagenetic conditions in the Severin nappe and Cosustea mélange south of the Cerna range and the Brebina fault (Fig. 5). The smectite content in illite was determined using air dry and glycolated specimens. The smectite content is temperature-dependent and the conversion of smectite into illite and the extent of reaction is used as an indicator of diagenetic to metamorphic grade (Frey 1987). Illite of the

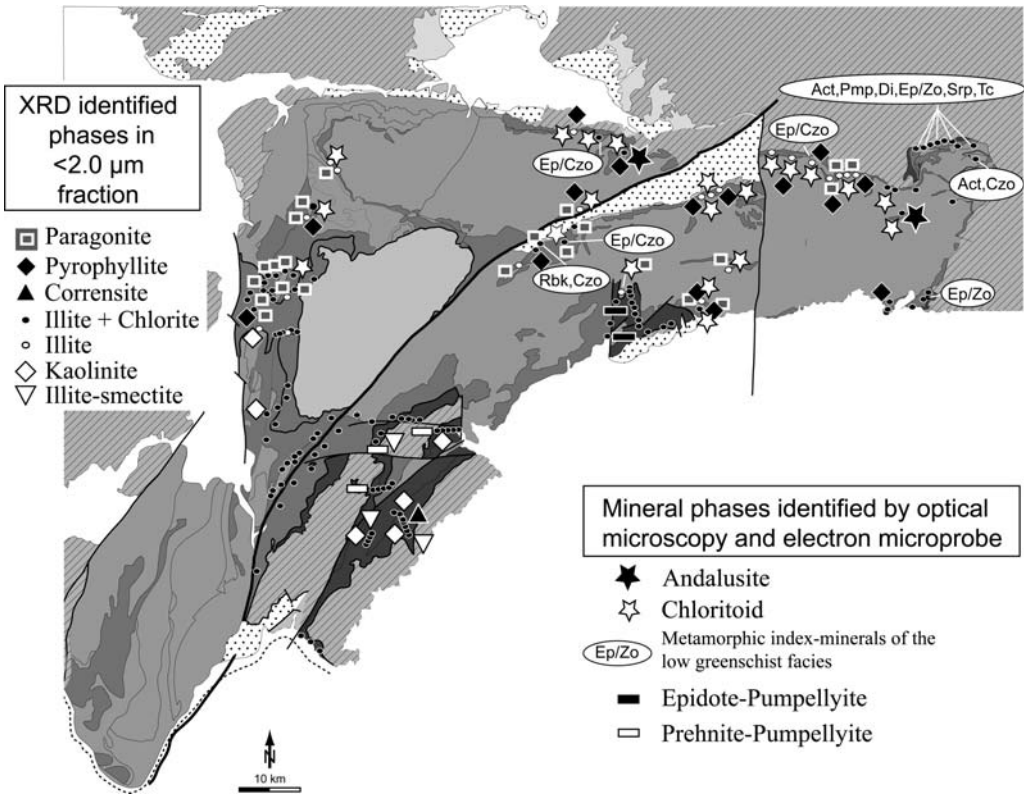


Fig. 5. Distribution of diagenetic and metamorphic mineral phases in Mesozoic sedimentary rocks of the Danubian window. The legend order reflects the increase in metamorphic grade from bottom to top. For mineral abbreviations (after Kretz 1983), see Bucher & Frey (1994) and the text.

diagenetic zone and low anchizone commonly show a marked asymmetry of the  $10 \text{ \AA}$  diffraction peak, with a low-angle tail, indicating the presence of expandable layers (Kübler 1967). In the high anchizone, the tail disappears. After glycol treatment, the smectite content in mixed-layer illite/smectite is recognized by a peak shift (due to swelling) to  $16.8 \pm 0.1 \text{ \AA}$ . Swelling of the smectite component leaves the  $10 \text{ \AA}$  reflection free of interference. Surprisingly, most samples also in the diagenetic zone were smectite-free.

North of the Godeanu outlayer and at Schela, north of Bumbesti (Fig. 2), chloritoid (Cld) was found (Fig. 5) in the Schela Formation. At these locations, and in the central part of the window, chloritoid rosettes and sheafs are preserved without deformation in massive mesoscopically unfoliated rocks. Mesoscopically also well-crystallized idioblastic chloritoid was found at Rafaila and the southern Tarcu range (Fig. 6b). In both areas, chloritoid is cross-cutting the slaty cleavage with lenticular aggregates of mineral grains (flaser structure) or a poorly developed schistosity

with mineral grains, which display a weak preferred orientation. The chloritoid shows a greenish to bluish pleochroism, a lamellar twinning and partly a zonation with a fainter pleochroic rim.

Along the southwestern border of the Petrosani basin (Fig. 2) and in the northeastern part of the Danubian window, colourless chloritoid crystals (Cld1) have also been observed, strongly deformed and partly syn-kinematically recrystallized (Cld2) within a second foliation (Fig. 6e).

Andalusite (And) was found in two samples of the Schela Formation rich in pyrophyllite and Al-white mica at the northern border of the Danubian window. North of the Petrosani basin (Fig. 5), microprobe observations revealed an aluminosilicate, presumed to be andalusite, intergrown between tabular chloritoid crystals in contact with quartz and pyrophyllite. In the backscatter image, this aluminosilicate is slightly darker in the grey scale than quartz, has euhedral crystals and a poikiloblastic texture. A second occurrence is situated in the Latorita range at Sasa Stefanu (Fig. 2) where poikiloblastic andalusite (Fig. 6c, d) was

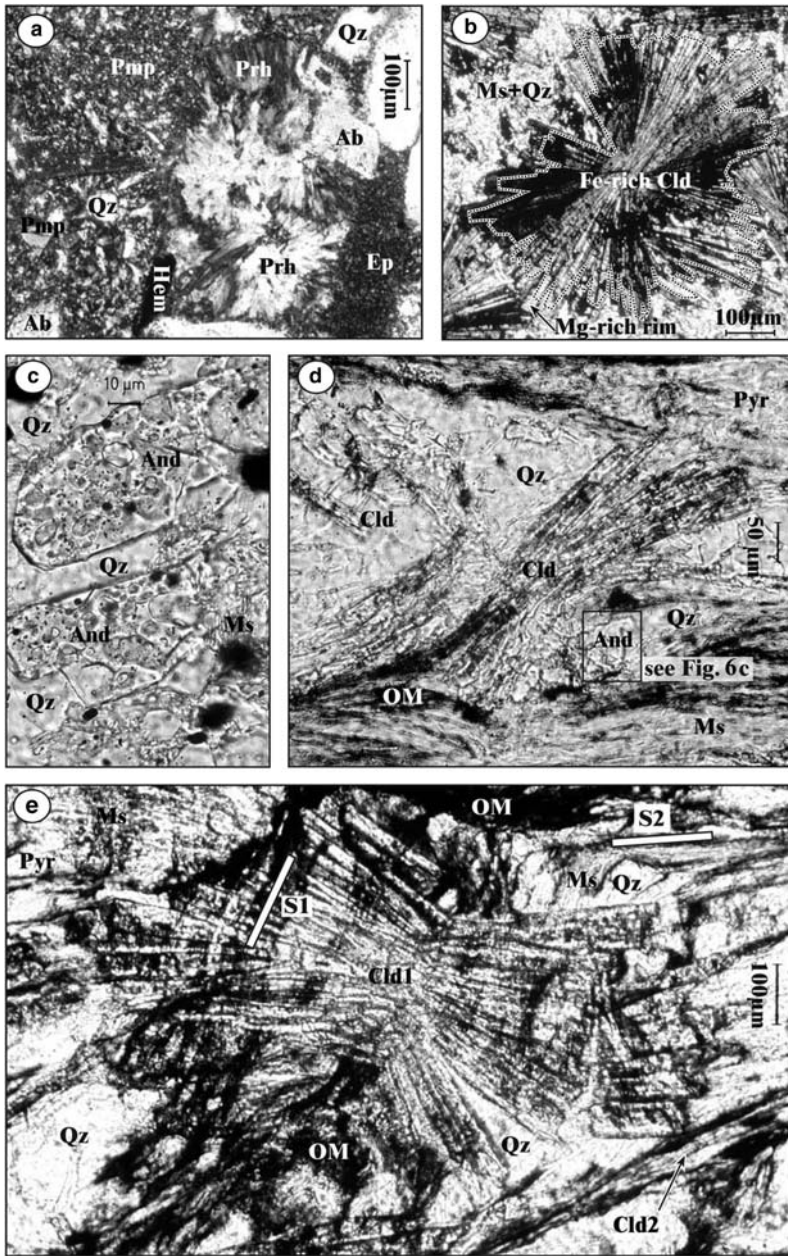


**Fig. 6.** (a) Prehnite (Prh) in an amygdule replacing plagioclase grains (Albite, Ab) occurring together with pumpellyite (Pmp) and epidote (Ep) in pillow basalt rocks of the prehnite–pumpellyite facies (sample 52 (Fig. 4) close to the Brebina fault). (b) Chloritoid (Cld) rosettes at Rafaila (Fig. 2, sample 219) well preserved without deformation in massive unfoliated rocks. In a combined optical and EMPA study, chloritoid shows a fainter pleochroic Mg-rich rim. (c) Poikiloblastic andalusite (And) at Sasa Stefanu (Fig. 2, sample 192) well identified by the high relief in quartz (see Fig. 6d). (d) Andalusite was identified in a quartz (Qtz) pressure shadow of chloritoid together with Al-rich muscovite (Ms). Pyrophyllite (Pyr) shows rotation and kinking and is part of the chloritoid mineral assemblage, but not in paragenesis with andalusite. A reaction involving andalusite is speculative. (e) Sample from the south of Petrosani (Fig. 2, sample 218) at Hotel Gambirinus, located close to the footwall of the Getic detachment. In the thin section, a rotated, deformed and broken chloritoid (Cld1) is shown. Organic matter (OM), sheet silicate and opaque mineral inclusions oriented in a parallel planar order reflect an old foliation ( $s_1$ ). The deformation of the Cld1 sheaf was caused by a second foliation ( $s_2$ ). The formation of quartz, muscovite and a second chloritoid generation (Cld2) in  $s_2$  is shown.

identified by optical microscopy in the pressure shadow of chloritoid (Fig. 6d), formed during deformation related to the Getic detachment. These represent the first occurrences of andalusite found in Al-rich Schela schists of the Southern Carpathians. No metamorphic kyanite or sillimanite was identified in the Mesozoic cover rocks. A blue amphibole was identified as *riebeckite* (Rbk) by EMPA (Fig. 5).

### *Metamorphic mineral associations from the Cosustea mélange and the Severin nappe*

The mineral association identified by XRD in the clay fraction from the Cosustea mélange, from the Azuga and Sinaia Beds of the Severin nappe consist of illite, chlorite, quartz, mixed white mica–paragonite minerals and rare albite. Intermediate peaks between paragonite and muscovite reflections in powder diffraction data are consistent with intimate mixtures of Na- and K-rich micas (Livi *et al.* 1997). These authors have shown in an HRTEM-work that the majority of these complex minerals are best described as domains and not as intercalation (*mixed layer K-mica/paragonite, sensu strictu* Frey 1969). Powder XRD spectra alone do not allow the determination of the exact nature of this metastable phase. Therefore, the name *mixed Na-K white mica* is suggested. Hematite is frequent in samples from the Azuga beds. Some other minerals were detected by transmitted light microscopy:

- *Prehnite* (Prh) is usually present as irregular vein fillings and amygdules (Fig. 6a), or it may replace plagioclase grains. Microscopic folds and/or faults overprinted some prehnite-filled veins. In the southwestern part of the window, prehnite occurs together with pumpellyite (prehnite–pumpellyite facies) in volcanic and volcanoclastic rocks. Prehnite1 is overgrown by fibro- to diablastic partly nematoblastic prehnite2 + pumpellyite + epidote2;
- *Pumpellyite* (Pmp) replaces plagioclase and clinopyroxene. Under prehnite–pumpellyite facies, also pumpellyite has been observed in amygdules (Fig. 6a), or as a relict phase, being broken and elongated along the schistosity and having a lenticular shape. Usually, pumpellyite is preserved only in the core of the crystals, while the rim is transformed to chlorite. In the northeastern part of the Danubian window, unaltered pumpellyite forms patches and is associated with newly formed actinolite (pumpellyite–actinolite facies) and sheet silicates (Fig. 5). In some volcanic rocks from the northeastern part of the Danubian window, granular aggregates of pumpellyite are overgrown by fibrous crystals of the same mineral. It is possible that

granular pumpellyite is cogenetic with yellow granular epidote, which is overgrown by colourless epidote–zoisite in the same samples;

- *Actinolite* (Act), together with chlorite, *epidote* (Ep) and pumpellyite, replaces clinopyroxene (augite–aegerinaugite) in gabbros from the northeastern border of the window. Actinolite may also be intergrown with clinozoisite. In gabbroic rocks and basalts, olivine and clinopyroxene are *serpentinized*. The colour and the needle-like habit suggest *antigorite* as the serpentine mineral (Srp, Fig. 5);
- *Zoisite/clinozoisite* (Zo/Czo) has been observed in the assemblage Act + Pmp + Chl + Ab + Ms + Kfs. In the northeast, Zo/Czo is found in pressure shadows related to the deformation of the Getic detachment, mostly in connection with relict feldspars. Euhedral plagioclase (also plagioclase in flysch rocks) and sometimes hornblende in the ophitic texture of the gabbros is partly saussuritized to epidote/clinozoisite + chlorite + albite. Granular epidote is partly overgrown by a colourless epidote–zoisite;
- *Diopside* (Di) occurs as a rim of relict clinopyroxene (Severin nappe, northern border of the Danubian window). Diopside is associated with Srp + Chl + Ep + Pmp + Act (Fig. 5); and
- *Chlorite* (Chl) occurs within volcanic and volcanoclastic rocks, both within the prehnite–pumpellyite and the pumpellyite–actinolite facies areas. However, chlorite is absent in many samples from the two Lower Jurassic formations, specifically at the northern border of the Danubian window (Fig. 5). The ultramafites are strongly serpentinized, and *talc* (Tc) is frequent. Epidote and clinozoisite are found in nearly all rocks of the northeasternmost part of the Severin nappe.

### *Mineral chemistry*

Microprobe analyses indicate that *pumpellyite* commonly found in Severin and Cosustea units is low in Fe. There is a decrease in FeO content, comparing samples from the prehnite–pumpellyite (FeO = 4.52 wt%) and the pumpellyite–actinolite association (FeO = 3.59 wt%).

The chemistry of *actinolite* in mafic rocks of the Severin nappe overprinted by pumpellyite–actinolite facies metamorphism varies between Mg/(Mg + Fe<sup>2+</sup>) ratios 0.69 and 0.81. A trend in chemical variation related to degree of metamorphism (e.g. Schmidt *et al.* 1997) cannot be detected since actinolite was only found at two localities.

Undeformed *chloritoid* rosettes from the central part of the window have an Mg-rich rim, MgO content increasing from 0.72 wt% in the core to 1.69 wt% on the rim (Fig. 6b). The

paragenesis is Ms ( $\pm$ paragonite) + Al-Chl + Qtz + Hem (Ti-Hem) + Pyr  $\pm$  Rt  $\pm$  Ep/Zo, and in rare cases paragonite and Fe-chlorite are formed at the expense of chloritoid. The same mineral assemblage without hematite is found at the northern margin of the window, where it is strongly deformed by a second schistosity (main foliation) as shown in Figure 6d and 6e. In many of these samples, chlorite is also missing. Chloritoid (ClD2) formed in the main foliation (Fig. 6e) is Fe-rich or has an iron-rich rim in many samples. Chloritoid in the main foliation may also be replaced by Ms (partly ferri-muscovite) + Al-Fe-Chl + Qtz  $\pm$  Ep ( $\pm$ Bt).

*Paragonite* (Pg) composition ranges from that of the Na-mica end-member to a low Na content in cases where interlayer positions are occupied by K-cations. Sometimes, interlayer positions are filled by similar amounts of Na and K. This probably represents a mica/paragonite interstratification (Frey 1969). Towards the muscovite end-member, the interlayer sheet composition is K-rich, still with a relatively high content in Na. No compositional trend as a function of metamorphic grade was found. Mostly paragonite occurs parallel to muscovite and often also parallel in the schistosity plane  $s_1$ . Here paragonite grows fibroblastic on muscovite in the shear sense and describes K-mica dissolution and Na-mica cleavage-parallel precipitation as shown by Livi *et al.* (1997).

*Chlorite* analyses, when plotted as non-interlayer cation versus Al, scatter along a line from close to clinocllore toward sudoite. In a chlorite Si-Fe<sup>2+</sup>-Al chemography, the analyses are situated between clinocllore and chamosite. No trend of chemical variation related to degree of metamorphism is evident. Also, the chemical composition gives no indication about a smectite contamination. The chlorite chemistry (Al-Si substitution) was used to determine temperatures with the 'geothermometer' proposed by Cathelineau (1988). Microprobe analyses of authigenic chlorites were normalized to 28 oxygens and fulfill the criterion  $\Sigma(\text{Na} + \text{Ca} + \text{K}) < 0.20$  constraining the contamination by other phases. Furthermore, all iron was assigned to Fe<sup>2+</sup>, because the electron microprobe does not distinguish between Fe<sup>2+</sup> and Fe<sup>3+</sup> (see also Cathelineau 1988). In recent years, chlorite 'geothermometry' has been used to determine palaeo-temperatures in sub-greenschist facies metamorphic rocks. According to Cathelineau (1988), the increasing tetrahedral Al content of trioctahedral chlorite is a function of increasing temperature. Schmidt *et al.* (1997) discussed the 'geothermometer' by a critical revision on the reliability. The decrease of tetrahedral Al in authigenic chlorites as a function of decreasing temperature can be explained by interstratification

of smectite with chlorite. TEM studies support this view (Schmidt *et al.* 1997). Interstratifications in chlorite were not detected by XRD analysis in the samples used. Nevertheless, the chlorite 'geothermometry' is interpreted with caution in this study.

*White mica* is ubiquitous in all samples analysed. White micas were normalized to 20 oxygens. In samples from the northeastern border of the study area, characterized by the high anchizone to epizone (see below), the interlayer cation content reaches values of 8.6 to 11 wt.% (1.45 to 1.9 atoms per formula unit (pfu)). The Si/2 ratio is 3.3 atoms pfu, and illites from the central part of the Danubian window show a ratio of 2.8 to 3.2 pfu. It is assumed that Si substitutes Al in the tetrahedral position as a function of pressure. Si content of white mica has been used to estimate pressure by applying the Massonne & Schreyer (1987) method only for those samples where the chemical composition indicated a phengitic component with a Si/2 ratio  $> 3.2$  pfu. However, because the assemblage phengite + K-feldspar + quartz + phlogopite is not present in our samples, the celadonite content has to be interpreted with caution. Detrital phengite in some samples show higher Si pfu values ( $> 6.8$  pfu).

#### *Illite Kübler index*

Cosustea mélange, Nadanova Beds, Azuga Beds and Sinaia Flysch (Severin-Cosustea unit) yielded KI values which indicate a trend (Fig. 7) ranging between the high diagenetic zone in the southwest at the Danube, the low anchizone at Bumbesti, the high anchizone at Polovraci and the epizone found in the northern and northeastern part of the Danubian window (in the Retezat range and at Voineasa). From a previous study, the trend is known (Ciulavu & Seghedi 1997). Intra- and intersample variations and petrovariances (dependency on the rock chemistry, Ferreiro Mählmann (1994)) decrease from the diagenetic zone to the anchi- and epizone from  $\text{KI} \pm 0.11$  to  $\pm 0.06$  and  $\pm 0.012 \Delta^\circ 2\theta$ .

Since samples from the Schela Formation in the Danubian nappes often contain paragonite and pyrophyllite, the (001) reflection of illite is frequently broadened (the presence of mixed-layer phases was not detected). In anchi- and epizonal illite-muscovites, the 2M<sub>1</sub> polytype predominates. In these cases, we used two methods to determine KI: (1) deconvolution of the reflection in the 10Å region; or (2) measurement of the FWHM of the (00,10) illite reflection. This latter reflection is not influenced by the presence of paragonite and pyrophyllite. The transformation of the values obtained for the (00,10) illite reflection into values corresponding to the (002) reflection was

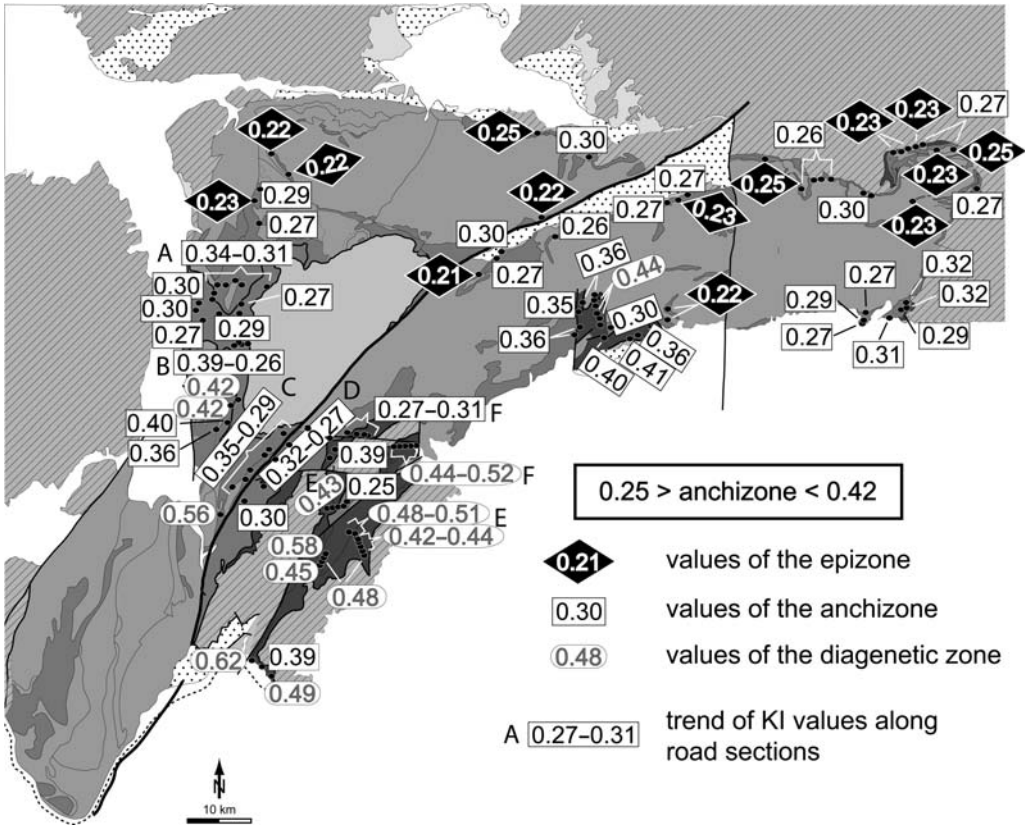


Fig. 7. Illite Kübler index (KI) map of the Danubian window. Values are indicated as Kübler index data  $\Delta^{\circ}2\theta$ . The anchizone limits are given by KI values based on a calibration with standards provided by Bernard Kübler and Martin Frey.

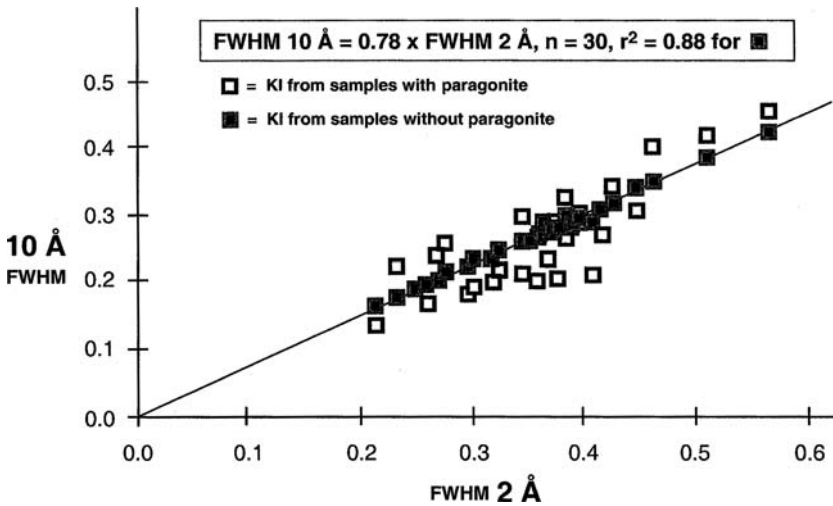


Fig. 8. Correction of illite Kübler index data (FWHM in  $\Delta^{\circ}2\theta$ ) using the transformation of the values obtained for the (00,10) reflection (2 Å) into values corresponding to the (002) reflection (10 Å). The (002) and (00,10) regression indicated is based only on those samples that lack an illite interference with paragonite and pyrophyllite.

achieved with an empirical regression equation, which correlates (002) and (00,10) reflections (Fig. 8). The results given by both methods are similar, although the values obtained by deconvolution are usually slightly lower (in the second decimal order).

In the area of the northern border of the Danubian window (Tarcul-, Retezat- and northern Latorita range, Fig. 2), the KI values obtained from samples with high organic matter content (determined from samples used also for VR) indicate both high anchizone and epizone conditions. However, the high anchizone values can be attributed to the retardation of illite aggradations. The organic matter forms a hydrophobic mantle around illite crystals, preventing them from aggradations (Frey 1987a). The organic coat is well recognized by reflected light microscopy around phyllosilicates. These samples were not used for the further study.

In the western area (Arjana nappe), diagenetic KI values in samples from the Ohaba Formation were found to be associated with the presence of paragonite and pyrophyllite. Both minerals are typical anchizone metamorphic index minerals (Frey 1987a). In general, in these samples the illite (002) reflection is very asymmetric, with a very long tail towards low  $2\theta$  angles, indicating the presence of an illite/smectite component. In the Ohaba Formation, gypsum is abundant and was probably produced by reaction between sulphuric acid with calcium. Sulphuric acid may result from pyrite weathering. An organic petrography study revealed that pyrite is transformed to an hydroxide. Organic matter is also strongly oxidized. This intense alteration is not visible in the hand-specimen due to the high organic content, which preserves the black colour of the sample. Low diagenetic values from these samples were not used for further correlation and therefore not shown in Figure 7.

Clays from the same area, intercalated in sandstones of the Ohaba Formation, show KI values of the epizone. Mesoscopically, a coarse detrital mica fraction is observed in these samples from the Arjana nappe (Fig. 2). To avoid an over-interpretation due to a possible detrital contamination, these samples were not used for further correlation and therefore not shown in Figure 7.

Using only pelites for a detailed study, most values show anchizone conditions. Along three road sections (10 samples each) at the east of the Godeanu outlayer, a KI decrease to the east is evident (A, B and C in Fig. 7). At the eastern margin of the window, the KI variation is  $0.34 \pm 0.06$  and at the outlayer it is  $0.29 \pm 0.03 \Delta^\circ 2\theta$ .

In spite of the difficulties regarding non-metamorphic influences on KI data from the

Lower Jurassic formations, the trend from the diagenetic/low anchizone in the southwestern part of the Danubian window towards epizone values for the northeastern parts is shown by the KI study in the Danubian nappes (Fig. 7). This metamorphic gradient indicated by the KI distribution pattern is disturbed across three tectonic structures:

(1) In Figure 7 at the south of the Godeanu outlayer (Fig. 2), diagenetic zone–low anchizone values west of the Cerna–Jiu fault show a SW to NE trend from KI 0.56 to 0.29  $\Delta^\circ 2\theta$  (road section C) and are juxtaposed with a KI trend from 0.33 to 0.27  $\Delta^\circ 2\theta$  at the east of this fault (road section D, Fig. 7). If the data uncertainty is taken into account, the discontinuity is not pronounced;

(2) A road section (section E) crosses from west to east the Getic outlayer at the south of the Brebina fault (Mehedinti klippen area). In the west, in the Danubian nappes, KI from 0.33 to 0.27 (section D) differs from KI values of  $0.39 \pm 0.03 \Delta^\circ 2\theta$  (5 samples) in the Cosustea mélange and  $0.43 \pm 0.02 \Delta^\circ 2\theta$  (5 samples) in the Severin nappe. In the Danubian nappes in the eastern footwall of the Getic outlayer, KI values of  $0.25 \pm 0.04 \Delta^\circ 2\theta$  (3 samples) differ again from KI values of 0.48 to 0.51  $\Delta^\circ 2\theta$  in the Cosustea mélange and 0.42 to 0.48  $\Delta^\circ 2\theta$  in the Severin nappe. The diagenetic zone values observed in Severin nappe and Cosustea mélange in the southernmost area contrast with the predominantly anchizone KI data obtained from the Schela Formation of the Danubian nappes. With a much smaller and not well-defined hiatus, a similar contrast is found between Cosustea mélange (KI = 0.44 to  $0.40 \pm 0.06 \Delta^\circ 2\theta$ , n = 10) and the Schela Formation (KI = 0.30 to 0.36  $\Delta^\circ 2\theta$ , n = 2) in an area close to Bumbesti; and

(3) The Brebina fault rather abruptly delimits the diagenetic zone (KI = 0.44 to 0.52  $\Delta^\circ 2\theta$ ) found in the Severin–Cosustea units to the south versus the anchizone to the north (KI = 0.27 to 0.31  $\Delta^\circ 2\theta$ , road section F, Fig. 7).

### *Organic matter reflectance (OMR)*

Organic matter reflectance measured on samples from the Schela and Ohaba Formations, the Cosustea mélange, and Palaeogene coals are shown on the map of Figure 9. The organic matter in pelitic siltstones of the Schela Formation consists of the following percentages of macerals:

- *vitrinite*: 0–20% in the west and south, 70 up to 80% in the east;
- *liptinite*: recognized by its characteristic shape: 2%;

- *inertinite*: (mostly semifuzinite + fuzinite ± macrinite ± micrinite): 40–50% in the west and south, 10% in the east;
- *bituminite*: 30–40%, in pelitic samples and coals from the western area (Ohaba Beds). In the southern areas, bituminite can yield much higher percentages. In the east, the bituminite content is between 10–20%. At high coalification stages, some bituminite varieties with a homogeneous anisotropic reflection can easily be mistaken for vitrinite (Koch 1997; Ferreiro Mählmann 2001). The trend towards more anoxic conditions towards the west and within the Ohaba Beds observed by Năstăseanu (1979) is confirmed in this paper.

Due to the low vitrinite content in the west and south of the Danubian window, bituminite was also considered for maturity determination. Solid homogeneous bituminite occurs as large reworked fragments, or was observed *in situ* in layers parallel to bedding (cata-bituminite). A homogeneous anisotropic variety can be used for maturity

studies and not only in diagenetic studies (Jacob & Hiltmann 1985; Jacob 1989) but also under very low-grade metamorphic conditions (Ferreiro Mählmann *et al.* 2001; Belmar *et al.* 2002). Solid bituminite is also found to fill pores or late veins (migra-bituminite), which cut through the host rock. In cata-bituminite-rich siltstones of the Schela Formation, vitrinite is sometimes strongly impregnated by migra-bituminite, as described by Radke *et al.* (1980) and Ernst & Ferreiro Mählmann (2004). This leads to bireflectance values, which are characteristic for bituminite rather than vitrinite (Wolf & Wolff-Fischer 1984; Ferreiro Mählmann 1994). This is well recognizable in coal seams at the mining locality of Schela (samples 21, 220) and in some samples west of the Godeanu outlayer. To avoid an over-interpretation due to a possible bituminite contamination, these samples were not used for further correlation and therefore not shown on Figure 9.

In the eastern part of the window, organic maturation was determined by VR measurements. Many samples, especially in the western part of the

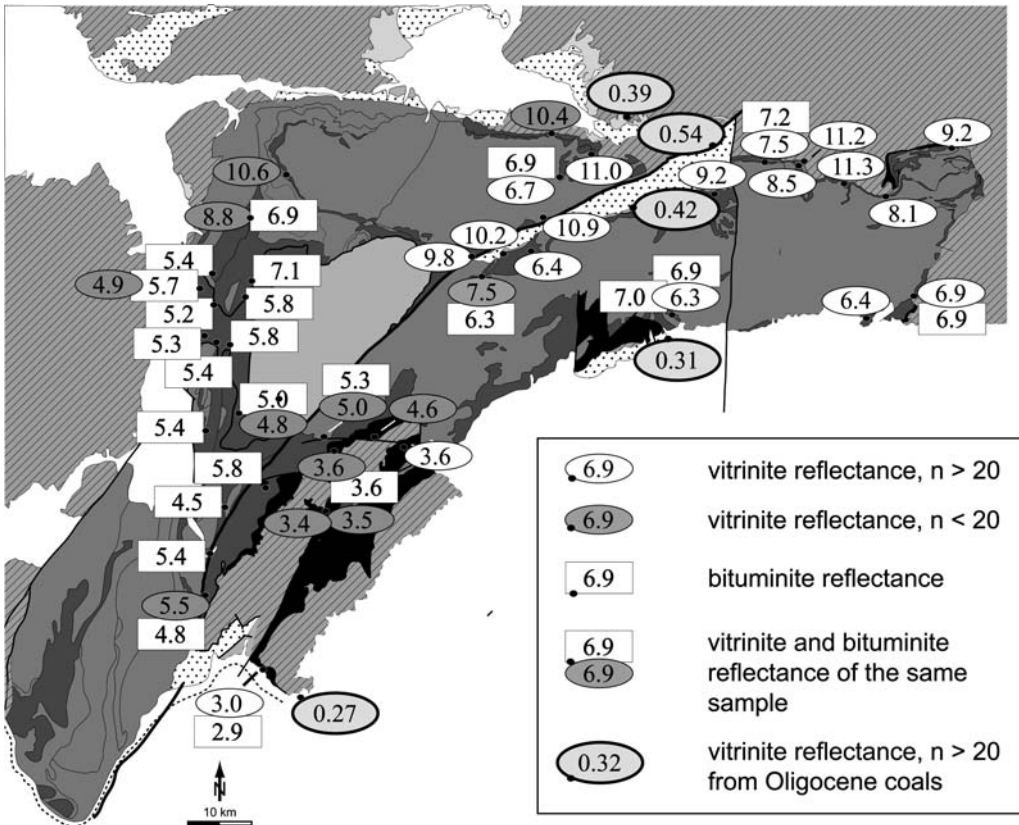


**Fig. 9.** Coalification map of the Danubian window based on vitrinite and bituminite reflectance %R<sub>max</sub> data (organic matter reflectance). The Oligocene coals are measured as R<sub>f</sub>%.

Danubian window, contained little or no vitrinite but abundant cata-bituminite. In the central and southern part also, only a few VR single values were obtained in one sample, but mostly the mean value is not statistically significant ( $n < 20$  measuring points,  $s_2 > 10\%$ , Fig. 9). Therefore, a correlation between vitrinite reflectance and cata-bituminite reflectance has been calculated on the basis of Schela samples, which contain both constituents (Fig. 10). In Figure 10, the values are superposed with the correlation given by Ferreiro Mählmann (1994, 2001). Cata-bituminite reflectance correlates well with vitrinite reflectance. Consequently, cata-bituminite reflectance (BR) is used for the evaluation of metamorphic grade. Due to the well-constrained correlation between VR and BR, the combination of the reflectance data will be denominated as organic matter reflectance ( $OMR \%R_{max}$ ).

In strongly sheared samples from the epizone, the organic matter yields much higher reflectance values compared to unfoliated rocks, and bireflectance is anormal. In shear zones,  $R_{max}$  reaches 9.0

to 12% for bituminite and 7.0 to 11.3% for vitrinite. These high reflectance values are due to the presence of pre-graphitic vitrinite and bituminite. Pre-graphitization, as described by Ramdohr (1928), Teichmüller (1987) and many others, was optically found (anisotropic or undulatory extinction and a high bireflectance, occurrence of rounded nearly submicroscopic spheres with poorly developed or no Brewster cross and helicitic extinction in cross-polarized light and graphitoid spheruliths). The highest VR were obtained in samples very close to the northern margin of the window deformed by the Getic detachment (Fig. 10). The detachment footwall is formed by mylonites, suggesting a strong influence of strain on the graphitization of organic matter (Bustin 1983; Teichmüller 1987; Suchy *et al.* 1997; Ferreiro Mählmann *et al.* 2002). At the east of Petrosani, a sample from a mylonite composed of Schela rocks (sample 205-1) shows a value of 11.2%  $R_{max}$ , a nearby sample in Schela schists (sample 205-2), only 100 m away from the mylonite, shows a VR of 8.5%  $R_{max}$ .

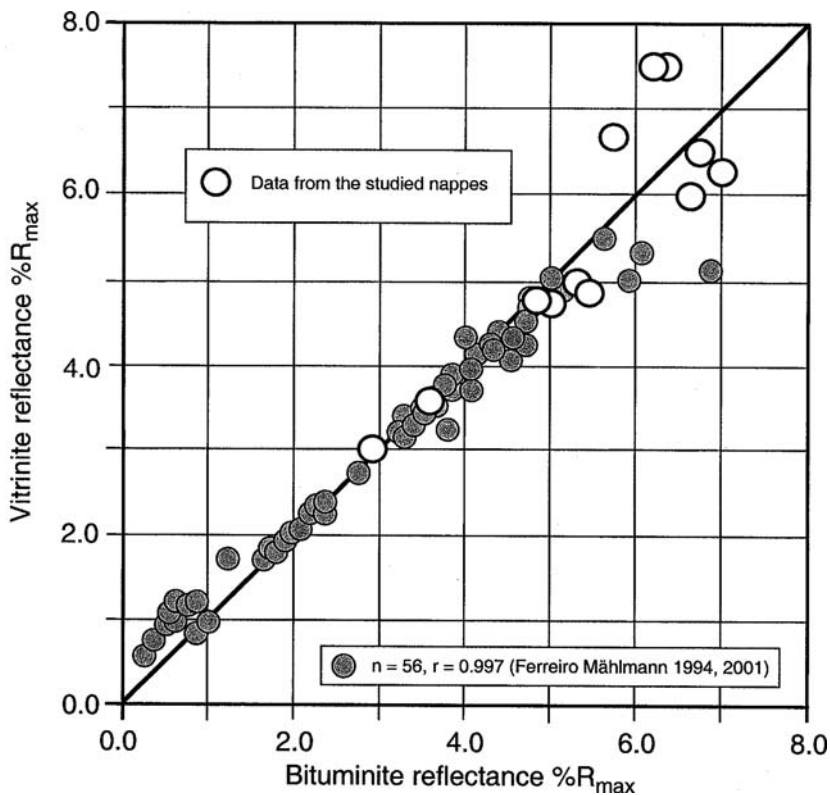


Fig. 10. Correlation diagram of vitrinite and bituminite reflectance. Between 1.5 and 5.0%  $R_{max}$ , both methods indicate the same rank of maturation.

All VR reflectance values of 9.2 to 11.3%  $R_{\max}$  are taken from ductile deformed and penetratively foliated detachment rocks and a strong maturity enhancement to  $>11\%$   $R_{\max}$  is found in mylonites (samples 203b, 205-1, 211, 215). The lowest peak in these samples with a bi- or polymodal distribution (Fig. 11c, d, sample 218 and 203b) is mostly around 7.5 to 8.5%  $R_{\max}$ . In less-foliated epizonal rocks from the same areas, values of 6.4 to 8.5%  $R_{\max}$  are found for bituminite and vitrinite. Therefore, the mean values of  $>8.5\%$   $R_{\max}$  close to the detachment do not reflect the grade of metamorphism.

In all parts of the Danubian window, a population with vitrinite reflectance of the meta-anthracite to graphite stage, found in several samples without oxidation, is distinguished as detrital organic matter (e.g. samples 206 and 207, Fig. 11a, b). This is best explained from sample 83 at the north of the Cerna range. A clay-rich foliated siltstone shows silt layers with abundant organic matter, giving a bimodal VR of 8.5 and 10.7%  $R_{\max}$ . In the clay-rich part, a unimodal peak is determined with a mean value of VR 5.0 and BR 5.3%  $R_{\max}$ . Few organoclasts show also values of 7.0 to 11.5%  $R_{\max}$ . Such detrital particles are rotated and have an inhomogeneous extinction; also maximum extinction is

not oriented parallel to the foliation or bedding. Usually, they are boudinaged and kinked.

In the epizonal part of the Danubian window, the difference between detrital and pre-graphitic particles (semi-graphite) is not visible due to a complete reorientation of organic matter. Also, the variance of the mean reflectance values of both vitrinite/graphite populations becomes more similar (Fig. 11d) making it impossible to discriminate between detrital and pre-graphitic populations in the reflectance histogram. From the diagenetic zone to the epizone (Fig. 11a, b) in a polymodal reflectance distribution, the lowest rank population is diagnostic for the determination of maturity and rock metamorphism. These populations were shown in the coalification map (Fig. 9). In the epizone, the histograms have a more unimodal shape.

In summary, an increasing metamorphic grade from southwest to northeast is indicated by the OMR data. However, again the distribution pattern is disturbed across three tectonic structures:

(1) the metamorphic discontinuity across the Cerna–Jiu fault is not well recognizable due to scarce OMR data. South of the Godeanu outlayer, an increase in BR from 4.5%  $R_{\max}$  in the west to 5.4 to 5.8%  $R_{\max}$  in the east is poorly constrained.

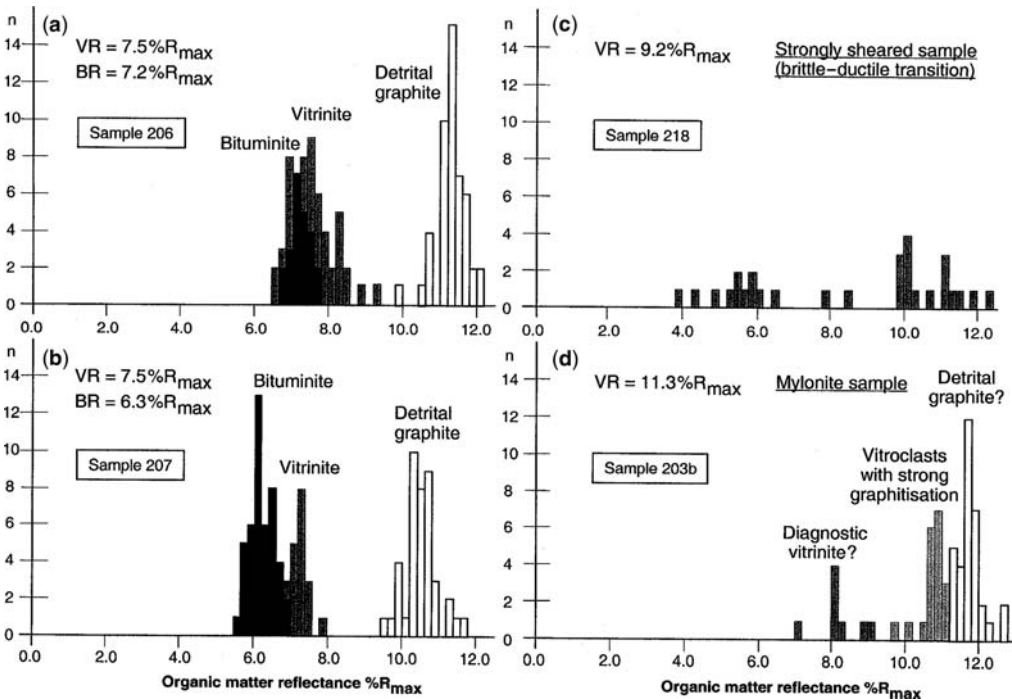


Fig. 11. Representative organic matter reflectance histograms from the Schela formation. From Figure 11a–d, an increase in deformation is indicated (from brittle to ductile). For discussion, see the text.  $n$  = absolute number of measurements.

Nevertheless, the change in rank of organic maturation is significant;

(2) The anthracite stage values found in Severin nappe and Cosustea mélange from the Mehedinti klippen (VR 3.0, BR 2.9%  $R_{max}$ , southern area and VR 3.4, 3.5, 3.6, BR 3.6%  $R_{max}$ , northern area) contrast with mostly high meta-anthracite data from the Schela Formation of the Danubian nappes (VR 4.8, BR 5.5%  $R_{max}$ , southern area and VR 5.0, BR 5.3, 5.8%  $R_{max}$ , northern area). A sudden increase in rank of organic maturation going across the tectonic contact between Severin nappe/Cosustea mélange and the Danubian nappes in the footwall is evident; and

(3) The zone of anthracite maturation in the south is abruptly limited by the Brebina fault towards the north. OMR values immediately north of this fault show a much higher reflectance (VR 4.6, 5.0, BR 5.3%  $R_{max}$ ) than values from the same tectonic unit at the south close to the fault (VR 3.6%  $R_{max}$ ) and further south (VR 3.6, 3.5, 3.4, BR 3.6%  $R_{max}$ ). The OMR data provide a significant argument to postulate a metamorphic hiatus coinciding with this tectonic structure (Fig. 9).

## Discussion

### *Correlation of metamorphic field trends and establishment of a metamorphic map*

*Illite Kübler index versus organic matter reflectance.* All data of this study, as well as published data on mineral assemblages (Stănoiu *et al.* 1988;

Ciulavu & Seghedi 1997) and FT data (Schmid *et al.* 1998; Bojar *et al.* 1998; Willinghofer 2000; Fügenschuh & Schmid 2005) indicate an overall increase in metamorphic grade from SW–NE.

The KI values obtained for Severin nappe and Cosustea mélange range from the diagenetic zone or lower anchizone in the southwest, up to the high anchizone in the east and finally to the epizone north and northeast of the Danubian window. Near the southern border of the Danubian window, KI values always remain anchizonal. Within the Danubian window, the Schela and Ohaba Formations yield high anchizonal to epizonal values along the northern rim of this window, but only anchizonal values along the western border and in the southern part. South of the Godeanu outlayer, some values indicating the diagenetic zone also occur. Overall, the trend given by the KI values is gradual but discontinuous across the Cerna–Jiu fault, across the Brebina fault and in the southern part also across the boundary between the Severin–Cosustea and Danubian nappe systems.

This same trend and discontinuities were confirmed by the measurements of OMR. High values were obtained in the northern and eastern parts of the Danubian window, the values decreasing towards the SW. The correlation between KI and OMR data (correlation coefficient,  $r^2 = 0.72$ ) is presented in Figure 12. The comparison with other IC/KI-VR/OMR, mostly linear regressions is not dependent from different VR measuring techniques,

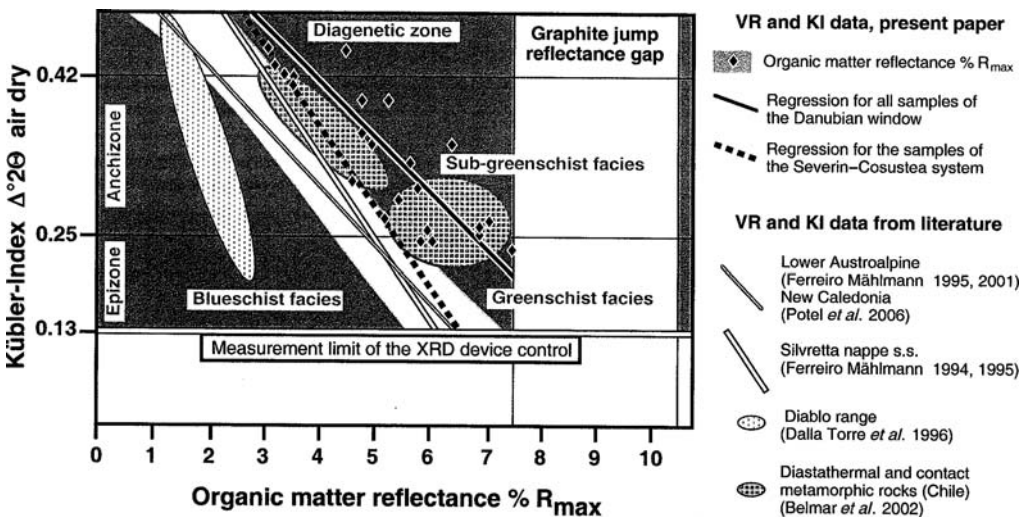


Fig. 12. Correlation diagram of organic matter reflectance and illite Kübler index values. The regressions for different sample groups from the Danubian window are compared with literature data (see text).

illite-calibrations and standardization procedures, because all studies cited were performed by the low-grade working group in Basel or by collaborating groups.

The KI-OMR regression line obtained for the Danubian window has a different slope and position compared to correlations obtained for samples from different tectonic units of the Alps and other areas (Fig. 12). In the white area of Fig. 12, all data of KI-VR correlations are integrated from studies in which the metamorphic imprint was generated by pressure and temperature conditions intimately related to LT–LP orogenesis (Frey *et al.* 1980; Krumm *et al.* 1988; Ferreiro Mählmann 1994, 1995, 1996, 2001; Rahn *et al.* 1994; Schmidt *et al.* 1997; Árkai *et al.* 2002). The area of orogenic diagenesis/metamorphism is limited by the 90% confidence boundary.

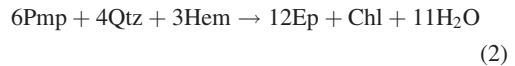
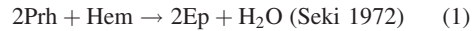
Correlation trends situated to the right side of this white area are derived from areas where high thermal gradient sub-greenschist to greenschist facies events were recognized (Krumm *et al.* 1988; Ferreiro Mählmann 1994, 1995; Belmar *et al.* 2002). Metamorphism is triggered by hyperthermal conditions as diastathermal-, contact-, hydrothermal- or ocean floor metamorphism. Correlation trends on the left side, however, comprise areas where hypothermal orogenic metamorphism is described ('high pressure sub-greenschist facies' conditions, Ferreiro Mählmann 1994; Petrova *et al.* 2002) and data from the Diablo range are characteristic for a blueschist facies event (Dalla Torre *et al.* 1996).

Steady-state equilibrium is documented in the Lower Austroalpine (Fig. 12) as shown by Ferreiro Mählmann (2001). With an identical regression, the one from New Caledonia (Potel *et al.* 2006) is given by a complete re-equilibration under normal-thermal conditions.

Compared with the correlation from the Lower Austroalpine and New Caledonia, that derived for the Danubian window points to enhanced VR all the way from the diagenetic zone to epizone (Fig. 12). Hence, on the basis of the previous discussion, this indicates 'high temperature gradient sub-greenschist facies' conditions. Furthermore, the data from the Danubian window are similar to those derived for samples from contact metamorphic rocks (Belmar *et al.* 2002). Note that samples from the Severin nappe and Cosustea melange give a regression line (Fig. 12) noticeably different from that composed by all samples of the Danubian window. The regression falls in the diagram on the right border of the white area related to orogenic (LT–LP) conditions (temperature-dominated). The slope is sub-parallel to that of the Silvretta nappe. A diastathermal regime describes Ferreiro Mählmann (1995) in the latter Alpine tectonic unit.

### *Sub-greenschist facies metamorphism of the meta-basalts*

The prehnite–pumpellyite facies (Fig. 14), restricted between 200 to 270 °C and 2.0 to 3.8 kbar (Frey *et al.* 1991), is characteristic for the volcanic and volcanoclastic rocks of the Severin–Cosustea nappe system adjacent to the southern part of the Danubian window (Mehedinti klippen) and is correlated with the zone of diagenesis (Fig. 13). In some samples, epidote is found together with prehnite and/or pumpellyite (Fig. 6a), post-dating an older Chl–Prh, Ep–Prh and Ep–Chl mineralization. The feldspars show no sericitization and are not partly saussuritized as is the case under epizonal conditions prevailing northeast of the Danubian window. The lower stability limit of epidote at low pressures <4.0 kbar is given at 200 to 220 °C (Seki 1972) by the following reactions, both possible in the study area (Fig. 6a):



Reactions (1) and (2) are found in the high diagenetic zone to lower anchizone, and OMR data indicate semi-anthracite to low anthracite coal rank.

In the northeast, in the basalts of the Severin nappe, the mineral association Ep + Zo/Czo + Pmp + Act + Chl + Qtz points to the pumpellyite–actinolite facies, which indicates temperatures in excess of 300 °C. Diopside was also identified in this area. The lower limit of the diopside stability field (Bucher & Frey 1994) also points to a minimum temperature of 300 °C. The maximum temperature is roughly estimated by the upper limit of the pumpellyite stability field at 250 to 350 °C (at 2 to 9 kbar, Frey *et al.* 1991).

### *The kaolinite-pyrophyllite reaction isograd*

The clay mineral fraction from pelitic rocks of the Schela Formation from the southern Danubian window consists of illite + chlorite ± kaolinite in the diagenetic zone. Additionally, mica/paragonite, pyrophyllite and Al-chlorite appear in the anchizone. In the northern and eastern epizonal parts of the Danubian window, pyrophyllite, paragonite, mixed-layer K-mica/paragonite or mixed Na–K white mica and chloritoid are frequently found (Fig. 5) as a typical assemblage of Al-rich pelites.

With increasing diagenetic to incipient anchizonal grade, pyrophyllite appears as the first index

mineral. The pyrophyllite (Pyr)-in isograd in the Danubian units is located west of the Godeanu out-layer. The reaction:



postulated for the western border of the window (Fig. 5) is pressure-independent (Hemley *et al.* 1980; Frey 1987*b*) but strongly dependent on water activity (Frey 1978). In Al-rich sediments, this reaction is reported at water in excess of temperatures  $\geq 260^\circ\text{C}$  (Fig. 14). Water in excess is indicated, as in the Danubian window, by the large amount of different phyllosilicates (Theye 1988) formed during metamorphism.

In contrast, based on a different kinetic approach, Iancu *et al.* (1984) and Iancu (1986) suggested metamorphic conditions of 390 to 420 °C at  $\text{PH}_2\text{O} = 2.0$  kbar for the Schela Formation, based on the same reaction  $\text{Kln} + 2\text{Qtz} \rightarrow \text{Pyr} + \text{H}_2\text{O}$ . These estimates of metamorphic conditions, also referred to in some recent papers, are too high for the following reasons:

(1) at 370 to 400 °C, the association  $\text{Ky} + \text{Cld}$  would be expected in pyrophyllite-rich rocks. Instead, we observed  $\text{And} + \text{Qtz}$ , indicating that the temperature was lower than 370 °C at pressures lower than 4 kbar (Fig. 14). Note that andalusite is found far away to the north of the pyrophyllite reaction isograd (Fig. 5), being part of a syn- to post-kinematic Getic detachment mineral association (Fig. 6c, d);

(2) the high content in organic matter suggests a water activity less than 1.0  $a(\text{H}_2\text{O})$ , which leads to a lowering of temperature for all dehydration reactions. Therefore, Frey (1987*b*) and Livi *et al.* (1997) give temperatures of 260 to 280 °C for the kaolinite-pyrophyllite association in the presence of  $\text{CH}_4$  or  $\text{CO}_2$  at  $a(\text{H}_2\text{O})$  of 0.6 to 0.9;

(3) pyrophyllite has been reported at the transition from the high diagenetic zone to the anchizone (Frey 1987*b*; Merriman & Frey 1999), but also at temperatures as low as 200 °C (Frey 1987*a*; Ferreira Mählmann 1994);

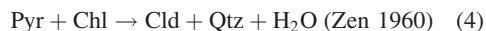
(4) based on new thermodynamic calculations, temperatures of more than 300 °C postulated by Thompson (1970) and Iancu (1986) with  $a(\text{H}_2\text{O}) \leq 1$  are unrealistic (Theye 1988). The assemblage  $\text{Ka} + \text{Chl} + \text{Ms} + \text{Qtz}$  is stable between  $a(\text{H}_2\text{O})$  0.5 and 1.0 below 3.5 and 5.5 kbar, but also temperature is strongly  $a(\text{H}_2\text{O})$  dependent. At an  $a(\text{H}_2\text{O})$  of 0.6, temperature is close to 240 °C (Potel *et al.* 2006); and

(5) kaolinite in the anchi- and epizone is related to a post-metamorphic P-T retrograde event. Some thin sections from the Schela Formation taken from localities close to the Petrosani basin

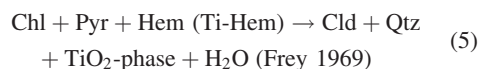
and along the Cerna–Jiu fault show fibrolitic, wool fibre-like or cloudy kaolinite aggregates between pyrophyllite and chloritoid. This is confirmed by microprobe studies and high magnification images obtained by HRTEM studies (David Schmidt, pers. comm.). The HRTEM study indicates that the kaolinite is newly formed between pyrophyllite layers and more abundant in screw dislocations, and in twin re-entrant angles of chloritoid were the potential of screw dislocations is amplified, providing suitable growth sites for kaolinite and some smectite. Feldspars were also altered to kaolinite.

### *The pyrophyllite-chloritoid reaction isograd*

In the Schela Formation from the northern epizone part of the area, chlorite is present only in 40% of the samples analysed. Chlorite is absent in those samples from the high anchizone to epizone, where both pyrophyllite and chloritoid are present in the clay fraction (Fig. 5). In samples 202, 203, 206b, 217, 219, 266 and 267 from the epizone, pyrophyllite is also missing. A breakdown of chlorite and pyrophyllite is well known for the epizone (Frey & Wieland 1975). This indicates that chlorite and pyrophyllite have probably been consumed by the reaction:



The chloritoid–chlorite thermometer (Vidal *et al.* 1999) could not be used due to the fact that chlorite is either entirely consumed in the above reaction or represents a post-chloritoid phase (see below). It is suggested that the initial sediments were Al-rich and poor in iron and magnesium. Based on thermodynamic calculations, a temperature of 300 °C (independent of pressure) is indicated for this reaction (Theye *et al.* 1996). Sometimes, hematite is still present in the same samples. At slightly higher grade (increasing VR up to values typical for the anthracite/meta-anthracite stage), the following reaction was observed by optical microscopy (Fig. 14):



Due to this reaction, rutile is formed in the Schela Formation. Theye & Seidel (1991) showed that chlorite reacts with hematite at about 310 to 320 °C and produces chloritoid, quartz and some magnetite. In the northern Latorita range, in the epizone (meta-anthracite/semi-graphite stage), bipyramidal opaque minerals are also found, the



when extrapolating the anchizone–epizone limit in Figure 13. Here, all metamorphic minerals are shown, independent of the chronology of their appearance. Hence the map only reflects maximum P–T conditions.

### Relations between metamorphism and deformation

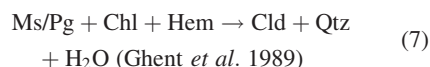
The base of the *Getic units* generally exhibits brittle deformation. In the northeast, syn-detachment deformation near the quartz brittle–ductile transition is restricted to the first ten metres. Within shear zones and specifically within the basement rocks near the Severin–Danubian boundary, a strong mineral banding, oriented parallel to the detachment foliation, is observed. Bands of (a) Ep/Czo + Chl, (b) Act + hornblende + Chl ± Qtz, and (c) Qtz + Ab/Plag ± Bt indicate syn-detachment greenschist facies conditions.

The metamorphic minerals of the prehnite–pumpellyite–epidote assemblage (Fig. 6a) from the *Severin-Cosustea unit* (Mehedinti klippen) were overprinted by the foliation related to the Getic detachment, or they were brittle deformed. The prehnite–pumpellyite facies assemblage is therefore pre-kinematic, and pre-dates the Getic extensional detachment.

In the Severin nappe of the northeastern part of the window, most minerals of the Act–Pmp–Di–Ep/Zo–Srp, Ep–Czo and Act–Czo assemblage + Cc–Qtz–Ap–Tc (Fig. 5) were affected by the detachment foliation and therefore also pre-kinematic to normal faulting. In samples exhibiting a strong detachment foliation, the mineral assemblage shows syn-kinematic deformation, as indicated by some pressure shadows, kinking of phyllosilicates, fragmented crystals and displacement-controlled fibres. A second generation of actinolite and epidote/clinozoisite is syn-kinematically formed. The feldspars were probably saussuritized synchronously. In a very few cases, both minerals, together with Fe-chlorite, cross-cut the detachment foliation and are associated with a late crenulation cleavage.

In the *Danubian units*, it is very difficult to evaluate metamorphic grades during Cretaceous nappe stacking and Palaeogene detachment formation separately. The mineral paragenesis Pg + Ms + Qtz + Cld found in the Tarcul range and at 'Rafaila' (Fig. 2) roughly indicates greenschist facies conditions. The minerals are well preserved with an idioblastic shape. Such undeformed assemblages are found in lower structural units, i.e. further away from the Getic detachment (samples 219, 266, 267). It can be thought that they were unaffected by deformation related to the Getic

detachment or that deformation diminishes with increasing depth (Fig. 17). It is also possible that higher temperatures prevailed during the detachment so that the paragenesis continued to recrystallize. Chlorite, hematite and pyrophyllite are missing in these samples (Fig. 6b), therefore also the following reaction, not involving pyrophyllite, can be assumed:



For the first time, blue riebeckite was found in one sample (Fig. 5), together with clinozoisite. Both minerals are affected by solutions related to the syn-detachment foliation. In some other samples, old rotated epidote/zoisite, chlorite and white mica were found. Chemical EMPA composition and thermo-barometric interpretation roughly indicate that temperatures of 300 to 350 °C and pressures around 3 to 5 kbar (Ms Si/2 (pfu) = 3.25 ± 0.05) prevailed prior to the detachment event. This is in good agreement with the chloritoid reactions (5) and (7) observed in some nearby samples (220, 218, 271). In summary, the mineral assemblage, the calculated temperatures, and the chloritoid (Cld1) formation reaction with and/or without pyrophyllite are probably related to a first greenschist facies and deformation event (Fig. 6e) that pre-dates the Getic detachment.

In the northern and northeastern Danubian window, greenschist facies conditions prevailed during the activity of the Getic detachment, since indicative mineral assemblages (samples 179 to 191) are stable within Getic detachment mylonites (Schmid *et al.* 1998). In syn-detachment micas, the Si content is commonly lower compared to that of the older and rotated micas, pointing to lower pressure conditions. In most cases, the mica is ferri-muscovite.

The thermal evolution during the Getic detachment can be only reconstructed in the Latorita range. In the other areas of the Danubian nappes, the results concerning P–T data related to pre-, syn- and post-Getic detachment stages are only scanty. Regarding the retrograde path (syn- to post-Getic), the occurrence of clinozoisite suggests temperatures >300 °C, while biotite + muscovite + chlorite indicate temperatures around 400 °C (Fig. 14). Hence, temperatures after chloritoid (Cld1) formation are slightly higher and evidenced by the syn-detachment Ep/Czo-Act/hornblende-Plag-Bt mylonites. Syn-detachment pressures of around 3 kbar, based on the phengite barometry (Ms Si/2 (pfu) = 3.20 ± 0.05) are indicated with caution for the northeastern border of the Danubian window. Andalusite formed along a

pressure retrograde path and limits the maximum pressure to 4.5 kbar (Bucher & Frey 1994) at the aluminium–silicate triple point, but to 3.5 kbar at 400 °C (Fig. 14).

After formation of the Getic detachment and during rapid cooling, post-Eocene fluid circulation and a low temperature hydrothermal activity is evidenced by the presence of small veins cutting the detachment-related deformation with  $Qz + Chl + Sm + Kln$ . Zones with an intense but very local kaolinization are revealed along the main Oligocene to Miocene faults and related to a relative high maturity of Oligocene coals (Fig. 9), specifically in the area around the Petrosani basin.

### Interpretation of metamorphic data

In the diagenetic zone (Fig. 13), between the Cerna range and the Danube (Fig. 2), mineral associations, including clay minerals, represent mostly a primary sedimentary or volcanic origin. Because the entire stratigraphic section (Permian to Cretaceous) occurs under metamorphic conditions all over the Danubian window, the lithologies of this area are used as reference for reaction educts.

#### *Metamorphic evolution of the Severin-Cosustea nappe system*

*Ocean-floor and Alpine metamorphism in the Mehedinti klippen area.* In basites and ultramafites of the Mehedinti klippen area, index minerals epidote + prehnite, chlorite + prehnite and chlorite + epidote are related to an old fabric. Epidote veins and amigdule fillings together with prehnite, chlorite, albite and also smectite, are remnants of a typical ocean-floor metamorphism (Robinson & Bevins 1999). The assemblages have been described in several earlier papers (e.g. Cioflica *et al.* 1981; Maruntiu 1987; Savu *et al.* 1985). However, diagenesis from the sedimentary rocks was high enough to overprint a burial KI and OMR trend. Rocks of different age at the same structural level show identical grade of diagenesis. In the slices of the ophiolitic-sedimentary sequence in the accretionary wedge, a top-down increase of diagenesis–anchizone metamorphism is not recognized. The increase of diagenesis and maturity to the northeast is a post-wedge tectonic trend within the Severin–Cosustea units.

Attempting a P–T determination, diagenesis cannot have been below 200 °C in the entire diagenetic zone studied since discrete smectite was not identified and liptinite and bituminite do not show a lower reflectance than vitrinite phytoclasts (Ferreiro Mählmann 1996, 2001). In the southern Mehedinti klippen area, pumpellyite was not

found; therefore we can conclude that minimum conditions for orogenic diagenesis are established at >200 °C, in agreement with reaction (1) and the formation of prehnite, not exceeding 2.5 kbar (point S-SC in Fig. 14, samples 94 to 96), in agreement with the epidote–phrenite stability field.

The prehnite–pumpellyite facies identified in sandstones from the Cosustea mélange and in basalts from the Severin nappe (point N-SC in Fig. 14, samples 52, 85, 87), is characteristic for the northern part of the Mehedinti klippen area (Fig. 5). Orogenic (Cretaceous) diagenesis (e.g. Manolescu 1937; Stănoiu 1972) has to be distinguished versus ocean-floor metamorphism (e.g. Maruntiu 1987; Savu *et al.* 1994). Ocean-floor relicts are again present in epidote veins and amigdules. Prehnite is overgrown by prehnite2 + pumpellyite + epidote2. The prehnite2–pumpellyite facies assemblage reflects re-equilibration to higher grade.

Pumpellyite is extremely rare from oceanic crust and related hydrothermal systems. Pressure is also generally too low for the stability of pumpellyite in mid-ocean ridge systems. This commonly results in the formation of prehnite + epidote (Frey *et al.* 1991; Alt 1999). Prehnite–pumpellyite facies is indicative for a LT-HP trend in the sub-greenschist facies (Frey *et al.* 1991) and typical in the LP zone (<4 kbar) for convergent settings (Alt 1999; Robinson & Bevins 1999).

KI data from the prehnite–pumpellyite facies in the northern part of the Mehedinti klippen area correspond to the diagenetic-/anchizone limit. Temperatures around 250 °C, based on the high diagenesis zone–anchizone temperature limit (Kisch 1987), are not very reliable due to the data uncertainty, but also kaolinite is present in nearby Al-rich samples (Fig. 5). Also the use of the chlorite thermometry is controversial, giving unrealistic high and inconsistent results, with a mean of 300 to 330 °C and variations in the range of  $\pm 50$  °C. Bulk rock chemistry, especially the Al/(Fe–Mg) ratios of rocks, strongly control the chemistry of chlorite (Árkai *et al.* 2002b). The original thermometer (Cathelineau & Nieva 1985) was elaborated for meta-andesites. Chlorite geothermometry values from pelites in the diagenetic zone often appear too high when compared with those indicated by the other methods (Schmidt *et al.* 1997) and should not be discussed, or with caution, at higher grade (De Caritat 1993).

In Figure 14, the southern (S-SC) and northern (N-SC) part of the Severin–Cosustea unit of the Mehedinti klippen are presented in a P–T diagram. The T °C estimation discussed were related with the Si (pfu) mica values as a first approach and plotted on the MP gradient of the

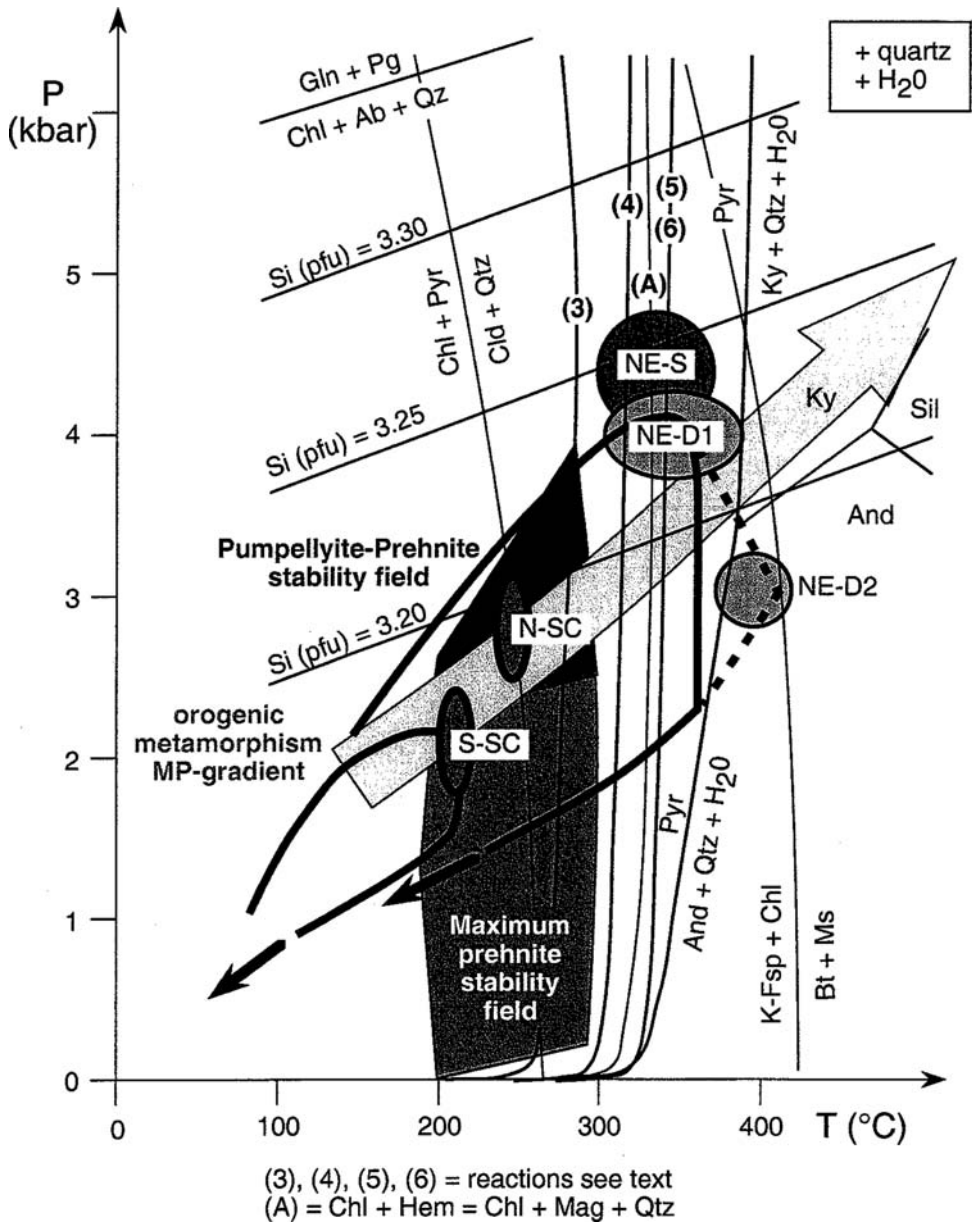


**Fig. 14.** Petrogenetic grid of the reactions found in the Danubian window. S-SC = southern part of the Severin–Cosustea nappe system; N-SC = northern part of the Severin–Cosustea nappe system (both at the south of the Godeanu outlayer); NE-S = northeastern Severin nappe; NE-D1 = Alpine conditions during the first deformation (nappe stacking) in the northeastern Danubian nappes; NE-D2 = conditions during and after the second deformation (Getic detachment) in the northeastern Danubian nappes. Shown also is the typical LT part of the orogenic MP path from Bucher & Frey (1994).

orogenic metamorphism path (Bucher & Frey 1994). The phengitic mica points to low pressures of <3.0 kbar, but mostly the mica is a ferri-muscovite. Muscovites with very small celadonite component cannot be used for pressure estimation.

With the available petrological and clay mineralogical data, a precise pressure determination is not possible.

On the basis that temperatures are around >200 °C (S-SC) and <250 °C (N-SC), VR/OMR

is 3.0 (S-SC) and 3.6%  $R_{\max}$  (N-SC), and pressures probably below 2.5 (S-SC) and 3.0 kbar (N-SC) a kinetic maturity and numerical model calculation for a better P-T approximation is used. The thermo-barometry proposed by Dalla Torre *et al.* (1997) was applied (see also Ernst & Ferreiro Mählmann 2004), combined for forward coalifaction simulation with the EASY% $R_0$  model from PDI-PC 2.2-1D (IES GmbH Jülich). From discussed field evidence, the diagenetic field gradient between S-SC and N-SC is synchronous in the klippen area. Therefore, the model is calibrated between the lowest temperature from S-SC and the highest from N-SC. In the OMR/VR-T °C plot (Fig. 15), the maturity range must fit with the temperature range from Figure 14. Pressure was calculated for a diagenetic interval of 1.0, 5.0, 10 and 15 million years. Below 5 million years, modelled temperatures are consistently too high to simulate OMR and above 15 million years pressures do exceed the stability field of prehnite and much above the Si/2 (pfu) 3.20 line (Fig. 14). The best fit results use 10 million years for modelling pressures of  $2.1 \pm 0.2$  kbar (S-SC) at 215 to 245 °C for 3.0%  $R_{\max}$  and  $2.6 \pm 0.2$  kbar (N-SC) at 245 to 265 °C for 3.6%  $R_{\max}$  (Fig. 15). The plotted ovals for S-SC and N-SC represent the range of error from measuring and modelling (Fig. 15).

In Figure 16, a very conservative approach is done using the EASY% $R_0$  model from PDI-PC 2.2-1D. Calibration as for the kinetic maturity model is applied. Additionally, burial during

sedimentation is modelled assuming a heat flow value of  $1.5 \text{ HFU} = 63 \text{ mWm}^{-2}$ . The sedimentary burial modelling step was very important to synthesize maturity in some Alpine nappes (Ferreiro Mählmann 2001; Árkai *et al.* 2002a). In the presented model, changes of  $\pm 5.0 \text{ mWm}^{-2}$  do not significantly influence the result, but during tectonic burial variations of  $\pm 1.0$  are much more important. During nappe stacking, a heat flow value of  $60 \text{ mWm}^{-2}$  was chosen, giving credit to a collisional scenario on the kyanite path (Bucher & Frey 1994). Time in the collisional part of the model is the main factor. At maximum depth, heating time during 10 million years is again proposed, reflecting the age determinations of 100 Ma (mica ages) and 80 Ma (zircon FT ages, see discussion for the Danubian nappes) and the results from the kinetic model. The EASY% $R_0$  PDI-PC 2.2-1D result is very similar to that of the kinetic model (Fig. 15) and the petrogenetic grid (Fig. 14). At 3.0%  $R_{\max}$ , temperature is 220 °C and eroded tectonic overburden is determined around 6 km (Fig. 16), therefore pressure should be 1.75 kbar for S-SC and 2.55 kbar for N-NC (8 to 9 km overburden).

The estimated metamorphic path shown in Figure 14 connecting S-SC with N-SC leads to a heat-flow path through the P-T field of 40 to  $60 \text{ mWm}^{-2}$  (Bucher & Frey 1994) and is therefore normal- to hypothermal.

The results obtained in this area show a coherent thermal pattern related to regional diagenesis post-dating ocean-floor metamorphism. The comparison

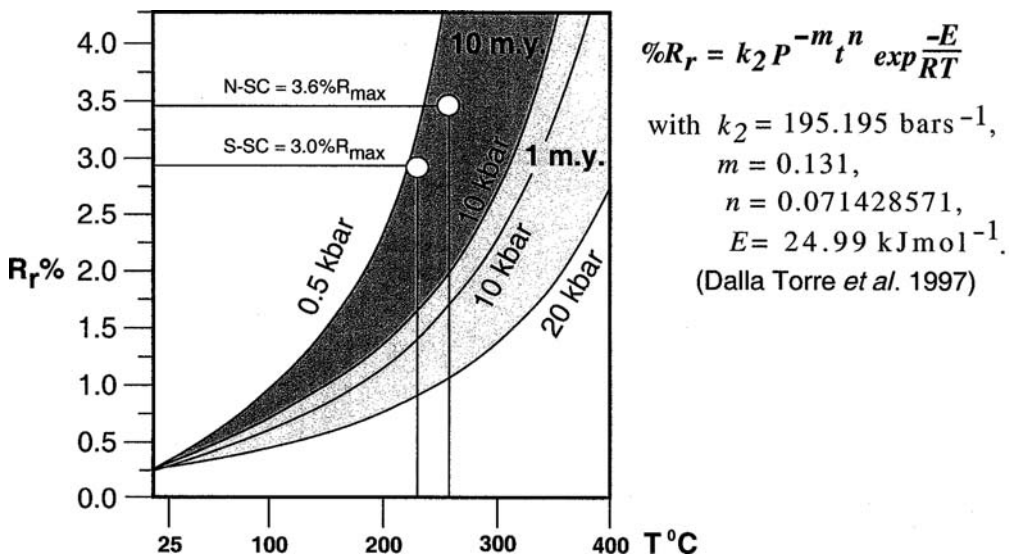


Fig. 15. Kinetic maturity model to substantiate the petrological and clay mineralogical study on Cretaceous metamorphism. For explanations, see text.

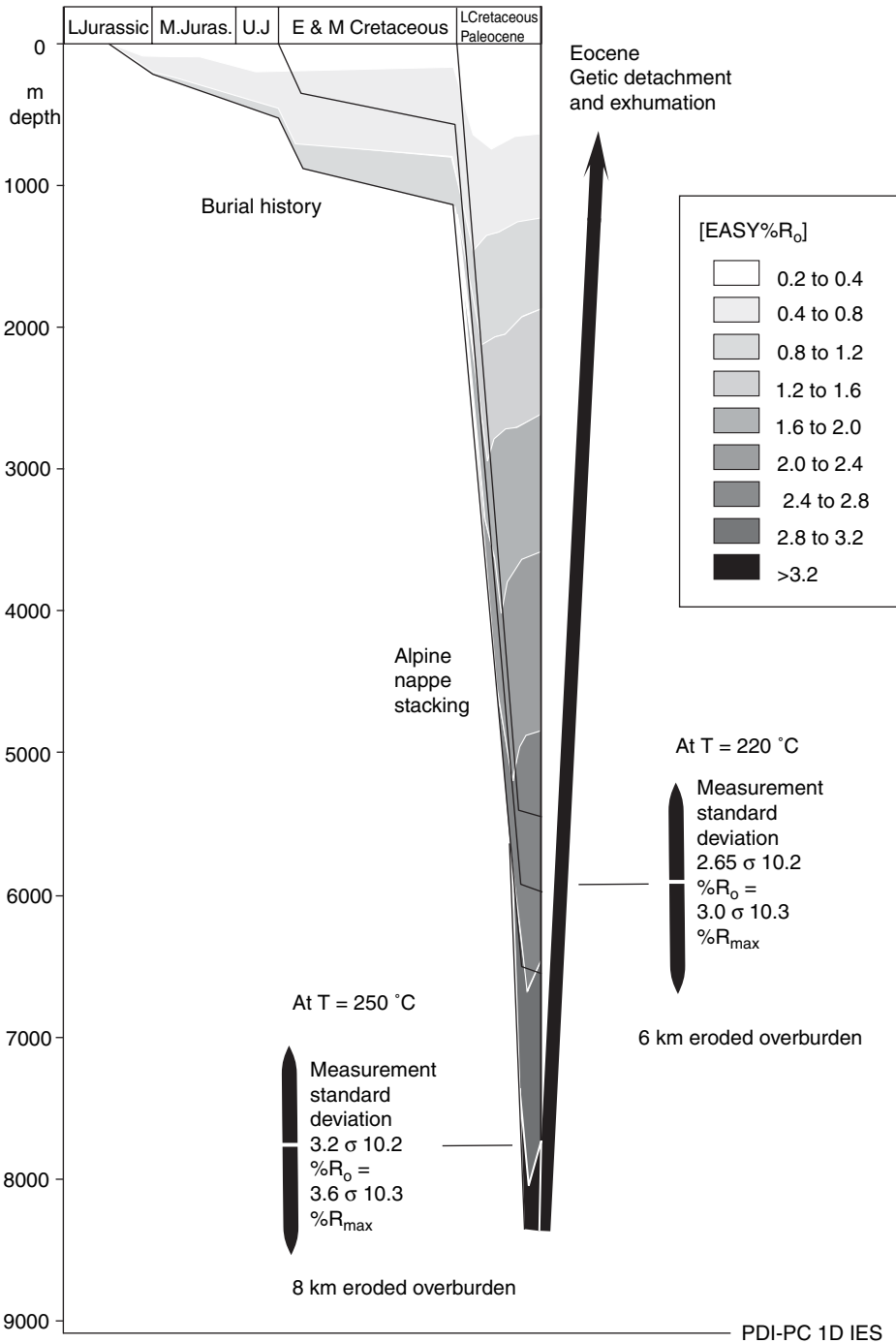


Fig. 16. EASY%Ro PDI-PC 2.2-1D (IES GmbH Jülich) basin evolution to nappe stacking model for the Mehedinti klippen area.

between grades of diagenesis, together with FT data on zircon (220 to 173 Ma) and apatite (55 to 50 Ma) from the very detailed study by Bojar *et al.* (1988) in the Mehedinti klippen area, suggest that an important Palaeogene orogenic thermal imprint did not affect the area south of the Brebina fault. Therefore, the indication by pumpellyite, together with the result that the values of OMR correlate with KI (Fig. 12), showing a typical trend for orogenic metamorphic conditions at LP on the kyanite path (Fig. 14), post-ocean floor metamorphism is related to Cretaceous Alpine orogeny. While the slope of the P–T path, defined by S–SC and N–SC, is typical for a LT–HP trend in the sub-greenschist facies between the kyanite and glaucophane P–T path.

*Subduction-related Cretaceous metamorphism in the eastern Severin–Cosustea unit.* While KI and OMR show an increase of metamorphism, the epidote + pumpellyite assemblage at Bumbesti (Fig. 5, samples 3, 5, 11 to 20) is not facies indicative and strongly dependent on  $fO_2$ ,  $a(H_2O)$ ,  $Fe_2O_3$  and whole rock composition (Potel *et al.* 2002). The lack of pyrophyllite and paragonite in clastic sediments, and also the lack of actinolite in volcanic rocks of the anchizone, indicate that metamorphism did not exceed 300 °C (Merriman & Frey 1999; Robinson & Bevins 1999) in this area.

At the northernmost corner of the Danubian window, the metamorphic mineral assemblages in the Severin nappe (NE–S) are partly deformed by the fabrics related to the Getic detachment, as is the case for the older granular population of pumpellyite. In case of the replacement of clinopyroxene by actinolite and diopside in gabbros, the relationship to deformation is not known.

For the ophiolite and flysch rocks, temperatures between 300 and 350 °C are roughly estimated from the Alpine mineral paragenesis as shown above. Chlorite in the s-c fabric of  $s_1$  in foliated volcanics (basalts–andesites to prasinites) give 310 to 345 °C using the chlorite thermometry. Chlorite thermometry from volcanic rocks of the epizone is in agreement with other temperature estimations as was found for the Severin nappe. Although the use of the chlorite ‘geothermometer’ proposed by Cathelineau (1988) for volcanics is uncertain when applied to meta-sediments, the temperatures obtained are often in good agreement with temperatures derived by other methods (Schmidt *et al.* 1997; Ferreira Mählmann 2001). In case of the pelite samples (mostly silty marls) from the Cosustea mélange and the Severin nappe, temperatures increase from 300 ± 20 °C at Bumbesti to 340 ± 20 °C in the eastern Latorita range. Chlorite found in the Nadanova beds of the same area indicates temperatures around 340 ± 20 °C. Chlorite2

in the syn-Getic detachment  $s_2$  fabric is not very frequent; the fabric is dominated by mica. A few temperature determinations show no significant difference to chlorite1.

For the older mica population, the phengitic mica ( $Si/2$  pfu > 3.23) points to pressures of ≥4.0 kbar (point NE-S in Fig. 14, see also Fig. 13). In general, the  $Si/2$  pfu differences of white mica indicate a relative pressure increase from southwest to northeast, but the celadonite content differs strongly in different samples. Pressure conditions during  $s_1$  based only on phengite barometry are not well established. Using the P–T estimate, the pre-Getic orogenic metamorphism was probably pressure dominated and is located in the P–T diagram (Fig. 14) at the transition of the HP greenschist to blueschist facies. Because of many uncertainties, the P–T area for NE-S is much larger than shown for S–SC and N–SC, but also reflects the same thermal path in the P–T diagram.

Comparing all areas studied in the Severin–Cosustea units, it is demonstrated that metamorphism post-dates ocean-floor metamorphism and sedimentary burial, but is pre-kinematic in respect to the Getic detachment. Hence it is a subduction-related sub-greenschist to greenschist facies Cretaceous metamorphic event (Seghedi *et al.* 1996; Ciulavu & Seghedi 1997) close to the glaucophane path, related to the ‘Austrian’ phase of the older literature (e.g. Stănoiu 1972). Based on radiometric ages of amphibole K/Ar-ages, biotite K/Ar- and Rb/Sr- ages, the metamorphic peak is dated at around 100 ± 10 and 110 ± 10 Ma (Ratschbacher *et al.* 1993; Grunefelder *et al.* 1993; Dallmeyer *et al.* 1996).

The increase of pressure with increasing metamorphic grade from south to north results in a subduction geometry to the north and an accretionary wedge thrusting top-south. Therefore, a Late Cretaceous nappe stacking top-south/southeast, as postulated by Schmid *et al.* (1998) and not top-east/northeast as reported by Ratschbacher *et al.* (1993) and Willingshofer (2000) is substantiated by the data of this paper.

Regarding the syn-detachment conditions in the northeastern part of the Danubian window, basalts from the Severin nappe show the following mineralogical association characteristic for the pumpellyite–actinolite facies: Chl + Ep/Czo + Ab + Act + Pmp + Qtz. The Zo/Czo + Pmp + Act assemblage, together with paragonite (determined by XRD), is typical for a HP transition (higher pressure bathozone) from sub-greenschist to greenschist facies (Robinson & Bevins 1999). The conditions did not change considerably, but the celadonite content in mica is much lower, indicating a pressure decrease from pre- to the syn-detachment metamorphism.

The replacement of hornblende by actinolite with epidote and rutile in syn-Getic mylonites (samples C, D and E) of the same area probably points towards higher pressures (Maruyama *et al.* 1986) than those expected for common greenschist conditions, or were controlled by oxygen fugacity and/or the bulk composition of the host rock. The transition from green hornblende to actinolite in the basement rocks may also indicate pressures decreasing to conditions  $<3.0$  kbar during the detachment, together with an increase in temperature (Black 1977; Sperlich 1988). A systematic geochemical study of the basement rocks has to verify this hypothesis.

### *Metamorphic evolution of the Danubian nappes*

*Accretion and nappe stacking.* For the transition from diagenetic zone to anchizone, temperatures of  $250^{\circ}\text{C}$  are inferred. The kaolinite–pyrophyllite reaction isograd (3) indicates temperatures  $>260^{\circ}\text{C}$ , probably around  $280^{\circ}\text{C}$  (Fig. 13, between samples 230 and 250) due to the high a ( $\text{H}_2\text{O}$ ) and the close vicinity of reaction (4).

The maximum metamorphic temperatures, such as indicated by reactions (4) and (5) in the Schela Formation of the Tarcul and Vilcanu range (Fig. 2), are between  $300$  and  $\geq 320^{\circ}\text{C}$  (Figs 13 and 14). Cooling in the west of the Cerna–Jiu fault is dated at 81 in the west to 51 Ma in the east (Willinghofer 2000; Fügenschuh & Schmid 2005). The reaction products (4) and (5) show deformation by  $s_2$  close to the Getic detachment but cross-cut the flaser structure or a poorly developed schistosity with also mineral grains displaying a weak preferred orientation  $s_1$ . Metamorphism occurred after last sedimentation in the Early Cretaceous and prior to cooling at 81 Ma. Cretaceous deformation  $s_1$  is related to nappe thrusting and the mineral paragenesis accommodated due to tectonic burial. Metamorphism can be related syn- to post-kinematic to the deformation during plate convergence posterior to the subduction of the Severin ‘ocean’ and collision of the Danubian continental block with the Getic–Supragetic units (Berza *et al.* 1994).

In the northeastern corner of the Danubian window, lower greenschist facies conditions (Stănoiu *et al.* 1982; Iancu 1986) in the semi-graphite stage (Popescu *et al.* 1982) at maximum temperatures of  $400^{\circ}\text{C}$  were also inferred by Ratschbacher *et al.* (1993) for the northeastern corner of the Danubian window. This assumption is not evidenced by mineral reaction in the  $s_1$  foliation. Relicts of the Cretaceous metamorphism (Pg1–Ms1–Chl1–Cld1–Czo1–Rbk) are typical

for Barrovian orogenic low greenschist facies metamorphism but an increase in metamorphic grade is not demonstrated. Relicts are found, as in the locality of Rafaila far away from the detachment (Fig. 17).

Only Ms1, Chl1 and Czo1 grow in many samples syn-kinematic in  $s_1$ . Therefore, the EMPA study was focused on the regional variations in the chemistry of Chl1 and Ms1.  $300$  to  $320 \pm 50^{\circ}\text{C}$  were obtained in Schela Formation samples from the north of the Petrosan basin (Retezat range, samples 212, 213) and in the northern Cerna range, increasing to  $350 \pm 30^{\circ}\text{C}$  in the Vilancu range (samples 3, 210) and in the northern Latorita range (samples 181, 189, 192) and  $350 \pm 50^{\circ}\text{C}$  at Schela (sample 21). In a Nadanova marl at Sasa Stefanu (sample 192b) from a homogenous composition analysis, a temperature of  $325 \pm 25^{\circ}\text{C}$  was calculated. The wide range of inferred temperatures is probably due to a detrital contamination, which is not recognized in the back-scatter image. Big crystals of probably detrital origin gave calculated values around  $400$  to  $450^{\circ}\text{C}$ . Compared with the other methods, the temperatures calculated are much too high in the Al-rich Schela Formation. The results confirm that the use of the chlorite ‘geothermometer’ proposed by Cathelineau (1988) for volcanites is unreliable when applied to Al-rich sedimentary rocks (Jiang *et al.* 1994). In case of Al-rich metapelites, a re-calibration of the temperature values is needed (Árkai *et al.* 2002b).

The result from the Nadanova marl may be close to realistic temperatures (see discussion related to samples from the Cosustea–Severin units). From phengite barometry, an increase of pressure from the Retezat range ( $>3.0$  kbar) to Schela ( $>4.0$  kbar) is evident on the same samples used for the Chl1 study. The Ms1 NW to SE trend may reflect the accretionary wedge geometry explaining increasing pressure with structural depth pointing to Late Cretaceous nappe stacking top-south/southeast, as postulated by Schmid *et al.* (1998).

*Getic detachment and syn-kinematic metamorphism.* Illite Kübler index, vitrinite reflectance, mineral associations and mineral chemistry, but also zircon fission-track (FT) data (Fügenschuh & Schmid 2005), all present the same trend, which indicates, different to that of  $s_1$ , an increase in metamorphic grade from southwest to northeast within the Danubian units. Shown by zircon FT ages, cooling started in the west in the Cretaceous and in the east during Palaeogene combined with a trend from partial to complete annealing (Fügenschuh & Schmid 2005). The clay mineral and maturity trends in the Danubian nappes, as

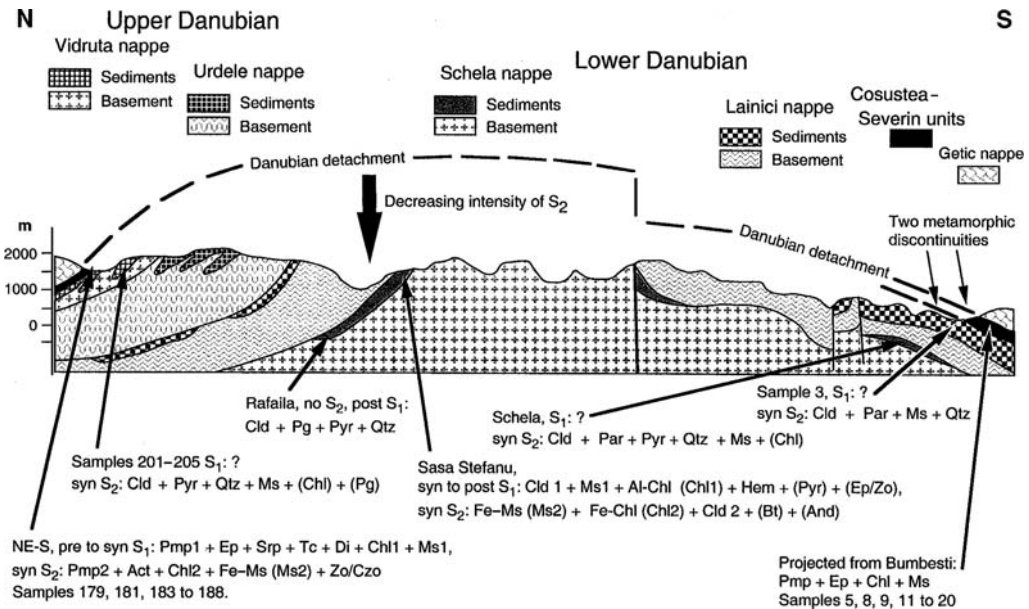


**Fig. 17.** Tectonic cross-section through the Danubian window at the east of the Sadu–Petrila fault with the metamorphic results from the Latorita range. Data from the Severin–Cosutea unit west of Bumbesti were projected into the section showing two progressive metamorphic discontinuities at nappe boundaries. Also the reason for preservation of Cretaceous Alpine conditions ( $s_1$ ) at a structural deep position at Rafaila is indicated. Getic deformation during  $s_2$  could not blur the Alpine fingerprint in Mesozoic cover rocks.

also the  $s_2$  mineral paragenesis, is distinguished by a different distribution pattern and not controlled by the structural level of the Cretaceous nappe system or topographic elevation.

The metamorphic pattern shown on Figures 13 and 17 cannot be related to a Cretaceous orogenic scenario, as shown in the last chapter, but was generally postulated (e.g. Mrazec 1898; Murgoci 1912; Manolescu 1937; Pop 1973; Berza *et al.* 1983), with a thermal peak during the Cenomanian to Turonian (Iancu *et al.* 1984; Berza *et al.* 1988a), and more recently dated at 100 Ma (Grünenfelder *et al.* 1983; Ratschbacher *et al.* 1993; Dallmeyer *et al.* 1996; Bojar *et al.* 1998). The main metamorphic pattern needs re-interpretation.

The lower temperature boundary of the anchizone at  $\pm 250^\circ\text{C}$  at the north of the Cerna–Jui fault (not found in the south of the fault) in the Danubian nappes is extraordinarily high (Fig. 13). In a collisional orogenic setting without magmatism, temperatures limit the anchizone in the range between  $220 \pm 20^\circ\text{C}$  and  $300 \pm 20^\circ\text{C}$  (Frey *et al.* 1980; Kisch 1987; Merriman & Frey 1999; Frey & Ferreiro Mählmann 1999; Ferreiro Mählmann 2001). The correlation between OMR and KI points to hyperthermal heat flow conditions and to a high thermal gradient sub-greenschist facies.

Data from Chl2 chlorite and Ms1 muscovite–phengite thermometry and barometry have to be discussed with the same caution as for the  $s_1$  study. The temperature calculations from Chl2, applied on the same samples, are in the identical range of error showing higher temperatures, but a higher standard deviation. In the marl sample 192a from Sasa Stefanu, a homogeneous Chl2 chemistry resulted in temperatures of 350 to  $400^\circ\text{C}$ . Regarding Ms2, the Si/2 (pfu) values scatter around 3.2 (most being lower and identified as ferri-muscovite). Only three samples (213, 220, 189) fulfil the criteria for the estimation, indicating 3.0 kbar in the Retezat range (identical to  $s_1$  conditions),  $<3.0$  at Schela and 3.0 at Voineasa. It can be inferred that the metamorphic temperatures during the Cretaceous evolution and during the Eocene Getic event were very similar while pressure decreased.

Cld1 formation is post-kinematic to Alpine nappe stacking (samples 219 at Rafaila, 266 and 267 in the Tarcul range) and pre- to syn-kinematic to the Getic detachment (northeastern Danubian nappes). In the  $s_2$  foliation, Cld2 is present from south of the Hatec basin to Voineasa, all along the northern margin of the Danubian window and in the epizone east of the Petrosani basin. In the Retezat Mountain and in the east and south of

Petrosani, reactions (A), (5) and (6) are defined from thin and EMPA sections. A temperature of  $>320\text{ }^{\circ}\text{C}$  is defined by these reactions in agreement with the minimum values of Chl2 thermometry (by accident?).

As described above, the neoformation of And + Bt + Chl + Ms (Fe-Ms) + Qtz in the pressure shadow of chloritoid (Cld1) was syn-kinematic to Cld2 within the schistosity related to the Getic detachment (Fig. 6c, d). K-Fsp in grain contact is also involved in the reaction (Fig. 14). It is possible that peak temperatures of 380 to 410  $^{\circ}\text{C}$  measured by chlorite thermometry and derived from Figure 14 were reached close to the end of the Getic detachment movement. This points to a temperature increase after Alpine orogenesis. Most data are in accordance with a P–T loop typical for a setting between orogenic collisional and HT-LP metamorphic conditions (Fig. 14) on the andalusite path. Maximum pressure (Cretaceous) and temperature (Eocene) were not reached simultaneously, but this is typical for all clockwise loops without isothermal decompression.

Under low-pressure conditions, OMR/VR is particularly dependent on temperature and time because the maturation of thermodynamically metastable organic matter is a mere expression of reaction rate (e.g. Hood *et al.* 1975; Waples 1980; Hunt *et al.* 1991; Ernst & Ferreiro Mählmann 2004). Therefore, the OMR can provide very important information about the thermal regime. The thermobarometry proposed by Dalla Torre *et al.* (1997) and Ernst and Ferreiro Mählmann (2004) could not be applied because for OMR  $>5.0\%$   $R_{\text{max}}$  kinetic modelling is not calibrated.

OMR is very high compared to KI and mineral paragenesis data. As deduced from Figures 12 and 14, the metamorphic imprint was dominated by a thermal event under low-pressure conditions and high heat flow. Comparing our data (Figs 12 and 13) with published data (e.g. Frey *et al.* 1980; Rahn *et al.* 1994; Ferreiro Mählmann 1994, 1996, 2001; Belmar *et al.* 2002), the high VR values (3.5 to 4.5%  $R_{\text{max}}$ ) at the upper limit of the diagenesis zone are associated with either hyperthermal ( $>70\text{ m W m}^{-2}$ ; Robert 1988) heat flow conditions or high geotherms ( $>35\text{ }^{\circ}\text{C km}^{-1}$ ). From the general correlation (Fig. 12), a VR value of 4.4%  $R_{\text{max}}$  is calculated, possibly indicating enhanced heat flow during the detachment evolution.

A short heating time is indicated by the fact that OMR suggests a higher metamorphism than that deduced from the corresponding KI values and the mineral assemblages. The retardation of mineral reactions and illite aggradation versus OMR, specifically under short thermal events or during short time with elevated heat-flux, is well demonstrated (see Wolf 1975; Teichmüller 1987; Barker

1989). A short heating time is also explained by the local detection of HT reactions and a poor mineral re-accommodation to the new P–T conditions. During crustal thinning in the South Carpathians and exhumation of the Danubian nappes, the chemical composition of minerals probably did not change and nearly no mineral neo-formation occurred. However, during the temperature increase, OMR was enhanced due to the high reaction rate of the organic maturation processes. The observed disequilibrium between KI, mineral paragenesis and OMR, similar to conditions known from contact metamorphic settings (e.g. Bostick 1973; Barker & Pawlewicz 1994; Elliot *et al.* 1999; Belmar *et al.* 2002), can only be preserved during a short time of temperature and/or heat flow increase.

The relatively elevated OMR in Danubian window can be well explained by isothermal decompression during the detachment related to a slight elevation of the geotherm due to crustal thinning and rapid exhumation of Danubian units. High heat flow can be enhanced by the rapid uplift of hot basement rocks with a high thermal conductivity. An elevated higher heat flux probably followed during maximum exhumation at the end of the Getic detachment, a time when the retrograde chloritoid decomposition reactions took place. During exhumation, heat flow increases to  $>150\text{ m W m}^{-2}$  during uplift of the Tauern dome (Fig. 1), as is well demonstrated by maturity studies (Sachsenhofer 2001). Thermal effects of exhumation of a metamorphic core complex on hanging wall syn-rift sediments were also well studied from the Rechnitz window (Fig. 1, Dunkl *et al.* 1998). The scenario demands a thermal influence to be considered in the Getic-Supragetic units. In this paper, it is evidenced: (1) by a ductile deformation of the basis of the Getic-Supragetic units in the northeast of the Danubian window (deformation is found in the first 10 m on top of the detachment Ep–Chl–Act–mylonites); and (2) by sediments on the Getic basement showing a high maturity. Coal seams and resedimented coal particles of Oligocene age were coalified to the sub-bituminous to high volatile bituminous stage at the southeast of the Hatec basin and in the Petrosani basin. In the area of Bumbesti and close to the Danube, the coal remains in the lignite stage (Fig. 9).

A slight increase in temperature in the Danubian nappes is supported in Figure 12 by the occurrence of andalusite and biotite (NE-D2). Fresh biotite, actinolite, blue-green amphibole and chlorite cross-cutting all microstructures are known from the basement rocks (Tudor Berza, pers. comm.). An initial increase of temperature is typical during the thermal evolution of a metamorphic core complex footwall (e.g. Genser *et al.* 1996; Dunkl

*et al.* 1998). An extremely rapid shortening combined with an advective heat transport causes an elevation of isotherms and thus the increase of near-surface geotherms (Koons 1987; Mancktelow & Grasemann 1997; Fügenschuh *et al.* 1997). Therefore, the main metamorphic pattern in Figure 13 is caused by a syn-Getic, Eocene metamorphism, and the Danubian window can be regarded as a very low- to low-grade high thermal gradient metamorphic core complex. Cooling below zircon annealing is determined for the Retezat and Vilcanu range at 64 to 54 and 67 to 46 Ma (Bojar *et al.* 1998; Schmid *et al.* 1998; Willingshofer 2000; Fügenschuh & Schmid 2005). East of the Sadu–Petřila fault, thermal metamorphism did not decrease below zircon annealing at 31 to 21 Ma (Fügenschuh & Schmid 2005). A much longer preservation of metamorphic conditions in this area may be the reason for establishment of equilibrium conditions in the microscopic scale and for identification of poikiloblastic andalusite (Fig. 6c, d) at Sasa Stefanu (Fig. 2) by optical microscopy together with biotite and chloritoid.

*Getic detachment and cooling history of the Danubian window.* Fission-track data from the literature (Fügenschuh & Schmid 2005) show three main trends: age decrease toward the north (east), towards lower tectonostratigraphic levels and towards the Tarcul–Retezat dome. The temperatures obtained in the northeastern part of the Danubian window confirm the temperatures in excess of 320 °C indicated by FT analysis (Schmid *et al.* 1998; Willingshofer 2000). These data emphasize a north(east)-ward-directed unroofing of the dome that was coupled with an increase in strain intensity at its northern margin (Bojar *et al.* 1998; Schmid *et al.* 1998; Willingshofer 2000; Fügenschuh & Schmid 2005).

In the Tarcul–Retezat dome, zircon FT data indicate cooling below 250 °C during the Campanian to Oligocene (Schmid *et al.* 1998). Therefore, the reactions (3) and (4) were of pre-Campanian age but post-nappe tectonic (Cenomanian to Turonian, Ratschbacher *et al.* 1993; Grünenfelder *et al.* 1983; Dallmeyer *et al.* 1996). In the east of the Cerna–Jui fault, cooling is much younger as determined by zircon data (Maastrichtian to Oligocene, Fügenschuh & Schmid 2005) and reactions (4), (5), (6) and (A) may have occurred later or reaction progress continued. Therefore, the zone boundaries on both sides of the fault do not need to be synchronous.

The trends shown by Figure 13 can be well explained by asymmetric extension, starting in the south(western) part of the Danubian window and propagating towards north(east). Asymmetric extension led to the rise of an asymmetric thermal dome, which results in higher temperatures for a

longer time in north(eastern) parts of the Danubian window (Fig. 14). In Figure 14, this is shown by thermal re-equilibration to NE-D2 instead of an isothermal decompression.

In the Mehedinti klippen area and at Bumbesti, a diagenetic–metamorphic discontinuity separates diagenetic to low anchizone rocks of the Severin–Cosustea system from hot high anchizone (Cerna range) to epizone rocks (Vilcanu range) of the Danubian nappes. The disturbed metamorphic pattern between Severin–Cosustea nappes and Danubian nappes can be explained by a progressive metamorphic hiatus (Fig. 17). A sudden P–T increase towards the footwall is typical for the displacement of a cool upper structural unit on a hotter lower unit along a normal fault. Probably normal faulting between the Severin–Cosustea system and the Danubian nappes is cogenetic with the Getic detachment.

In the Mehedinti klippen area and at Bumbesti, the ocean-floor metamorphism and the diagenetic to anchizone metamorphic pattern related to Cretaceous nappe stacking in the Severin–Cosustea system was preserved and remained unaffected by the hyperthermal Getic low-pressure event documented for the central and northern part of the metamorphic core complex. The normal faults caused a displacement of the higher nappes towards the southeast, to the extremity of the dome. Consequently, this area escaped the high heat flux in the central part of the dome and the stage of the Alpine KI-VR equilibrium (note the different trend in Fig. 12) was not altered.

## Conclusions (geochronology)

(1) Jurassic ocean-floor (prehnite–epidote facies) and Cretaceous collisional orogenic metamorphism (prehnite–pumpellyite facies in the southwest to pumpellyite–actinolite facies/incipient HP greenschist facies in the northeast) is constrained in the Severin–Cosustea nappe system. The trend in increasing metamorphic grade is related to a subduction geometry top-north/northwest. Due to the metamorphic discontinuity at the base of the Cosustea wildflysch and Severin nappe in the Mehedinti klippen area and the displacement to southwest by a normal fault (probably a syn-Getic detachment fault), the Jurassic and Cretaceous metamorphic high diagenetic conditions were also not blurred in sedimentary rocks by the Maastrichtian to Oligocene thermal event.

(2) Two steps in the Cretaceous metamorphic path can be distinguished. The peak metamorphic conditions in the syn-nappe stacking epizone of the subducted Severin unit are close to those of the blueschist–greenschist transition. Also the syn

$s_1$  (first deformation) metamorphism in the Danubian nappes appears characteristic of LT-HP collisional orogenic conditions between the kyanite and glaucophane path. Peak pressure conditions  $\geq 4$  kbar in the structural lowest units under sub-greenschist to greenschist facies were reached in the Mesozoic cover during top-southeast Cretaceous nappe stacking. The accretional wedge was formed during Cenomanian to Turonian time.

(3) In the west of the Cerna–Jiu fault, reaction isograds and the diagenetic to metamorphic zone-boundary pattern are established due to metamorphic accommodation after nappe thrusting (diagenesis to greenschist facies, diagenetic zone to epizone). Metamorphic conditions indicate an increase in heat flow and temperature, related to an early stage of Getic detachment movements in the Senonian. Cooling started at Maastrichtian time. The metamorphic pattern is re-equilibrated between the Cenomanian and Maastrichtian.

(4) In the east of the Cerna–Jiu fault peak temperature conditions were reached during or slightly after formation of the Eocene Getic detachment. Decompression during the detachment event caused a high thermal gradient greenschist facies metamorphism with the characteristics of hyperthermal conditions between the kyanite and andalusite path, but far away from a contact metamorphic path. This is best explained with crustal thinning and exhumation, because no magmatism is known. Cooling followed in the west during Maastrichtian and Palaeocene time and in the east during the Eocene and Oligocene. In this area, reaction progress may have continued until the Oligocene.

(5) Crustal thinning is located between the Getic–Supragetic nappes and the Severin–Cosustea nappes. However, part of it must be located between the Severin–Cosustea nappes and the Danubian nappes. The amount of missing crust increases from the southwest to the north and northeast indicated by the metamorphic progressive discontinuity between the foot- and hanging wall of the detachment and at the normal fault below the Mehedinti klippen area.

(6) Oligocene to Miocene faults (Cerna–Jiu, Brebina) disturb the metamorphic pattern in the Danubian window. A very low-grade hydrothermal event is related to Oligocene–Miocene faulting.

We thank Susanne Th. Schmidt and Willem B. Stern for their introduction to microprobe and X-ray diffraction work, respectively. B. Fügenschuh is thanked for his cooperation regarding comparisons with fission-track data. David Schmidt is thanked for HRTEM analyses. Our work benefited from discussions with Tudor Berza who generously shared with us his comprehensive knowledge regarding the Danubian window. M. C. thanks Sebastián Potel and Mauricio Belmar for their help during the last years. R. F. M. thanks Patrik Mathys

and Ulrich Szagun for their kind help in terms of computational support. We also thank Ronan Le Bayon for trying several thermodynamic calculations on chlorite and chloritoid. Willy Tschudin, our patient expert, prepared our thin and polished sections. The Swiss National Science Foundation is thanked for financing the project through Research Grant for the Cooperation in Science and Research with Central and Eastern European Countries: CCES/NIS joint research project No. 7RUPJ048623 and for support through SCOPES 2000–2003 project 7RUPJ062307. RFM wants to note that the project benefited very much from the extraordinary good relation between structural geologists and metamorphic petrologists in Basel; therefore, the political decision to close geosciences is very tragic. The authors are grateful to two anonymous reviewers of the first manuscript, but deeply indebted to Prof. Peter Arkai for critical reviewing and constructive corrections and suggestions. Thanks are extended to PD Dr. Ulrich Glasmacher for very helpful comments.

## References

- ALT, J. C. 1999. Very low grade hydrothermal metamorphism of basic igneous rocks. In: FREY, M. & ROBINSON, D. (eds) *Low-Grade Metamorphism*, Blackwell Sciences, Oxford, 169–201.
- ÁRKAI, P., FENNINGER, A. & NAGY, G. 2002a. Effects of lithology and bulk chemistry on phyllosilicate reaction progress in the low-T metamorphic Graz Paleozoic, Eastern Alps, Austria. *European Journal of Mineralogy*, **14**, 673–686.
- ÁRKAI, P., FERREIRO MÁHLMANN, R., SUCHY, V., BALOGH, K., SYKOROVA, I. & FREY, M. 2002b. Possible effects of tectonic shear strain on phyllosilicates: a case study from the Kandersteg area, Helvetic domain, Central Alps, Switzerland. *Schweizerische Mineralogische und Petrographische Mitteilungen*, **82**, 273–290.
- BARKER, C. E. 1989. Temperature and time in the thermal maturation of sedimentary organic matter. In: NAESER, N. D. & MCCULLOH, T. H. (eds) *Thermal History of Sedimentary Basins. Methods and Case Histories*. Springer, Heidelberg, 73–98.
- BARKER, C. E. & PAWLEWICZ, M. H. 1994. Calculation of Vitrinite reflectance from thermal histories and peak temperature: A Comparison of methods. *American Chemical Society Symposium*, 216–229.
- BELMAR, M., SCHMIDT, S. T., FERREIRO MÁHLMANN, R., MULLIS, J., STERN, W. B. & FREY, M. 2002. Diagenesis, low-grade and contact metamorphism in the Triassic–Jurassic of the Vichuquen–Tilicura and Hualane–Gualleco Basins, Coastal Range of Chile. *Schweizerische Mineralogische und Petrographische Mitteilungen*, **82**, 375–392.
- BERZA, T. & DRĂGĂNESCU, A. 1988. The Cerna–Jiu fault system (South Carpathians, Roumania), a major Tertiary transcurrent lineament. *Dari de Seama ale Sedintelor Institutul Geologie si Geofizica*, **72**, 43–57.
- BERZA, T., IANCU, V., BALINTONI, I. ET AL. 1994. Excursions to South Carpathians, Apuseni Mountains and Transylvanian Basin. Description of stops, *Field Guidebook ALCAPA II, Romanian Journal of Tectonics and Regional Geology*, 105–146.

- BERZA, T., KRAEUTNER, H. G., DIMITRESCU, R. & ANON. 1983a. Nappe structure in the Danubian Window of the central South Carpathians; Travaux du douzieme congres de l'Association geologique Carpatho-Balkanique. *Anuarul Institutului de Geologie si Geofizica (Annuaire de l'Institut de Geologie et de Geophysique)*, **60**, 31–39.
- BERZA, T., SEGHEDI, A. & ANON. 1983b. The crystalline basement of the Danubian units in the central South Carpathians; constitution and metamorphic history; Travaux du XIIeme congres de l'association geologique Carpatho-Balkanique; Metamorphisme-magmatisme-geologie isotopique. *Anuarul Institutului de Geologie si Geofizica (Annuaire de l'Institut de Geologie et de Geophysique)*, **61**, 15–22.
- BERZA, T., SEGHEDI, A. & DRĂGĂNESCU, A. 1988a. Unitățile danubiene din versantul nordic al muntelui Vilcan (Carpați Meridionali). *Dari de Seama ale Sedimentelor Institutului Geologie si Geofizica*, **72**, 23–41.
- BERZA, T., SEGHEDI, A. & STANOIU, I. 1988b. Unitățile danubiene din partea estică a muntelui Retezat (Carpați Meridionali). *Dari de Seama ale Sedimentelor Institutului Geologie si Geofizica*, **72**, 5–22.
- BLACK, P. M. 1977. Regional high-pressure metamorphism in New Caledonia; phase equilibria in the Ouegoa District. *Tectonophysics*, **43**, 89–107.
- BOJAR, A. V., NEUBAUER, F. & FRITZ, H. 1998. Cretaceous to Cenozoic thermal evolution of the southwestern South Carpathians: evidence from fission-track thermochronology. *Tectonophysics*, **297**, 229–249.
- BOSTICK, N. H. 1973. Time as a factor in thermal metamorphism of phytoclasts (coaly particles); Septieme Congres International de Stratigraphie et de Geologie du Carbonifere. *Compte Rendu Congres International de Stratigraphie et de Geologie du Carbonifere (International Congress on Carboniferous Stratigraphy and Geology)*, **7**, 183–193.
- BUCHER, K. & FREY, M. 1994. *Petrogenesis of Metamorphic Rocks*. 6th edn. Heidelberg, Springer Verlag.
- BUSTIN, R. M. 1983. Heating during thrust faulting in the Rocky Mountains; friction or fiction? *Tectonophysics*, **95**, 309–328.
- CATHELINEAU, M. 1988. Cation site occupancy in chlorites and illites as a function of temperature. *Clay Minerals*, **23**, 471–485.
- CATHELINEAU, M. & NIEVA, D. 1985. A chlorite solid solution geothermometer. The los Azufres (Mexico) geothermal system. *Contributions to Mineralogy and Petrology*, **91**, 235–244.
- CIOFLICA, G., SAVU, H., NICOLAE, I., LUPU, M. & VLAD, S. 1981. Alpine ophiolitic complexes in South Carpathians and South Apuseni Mountains. *Carpatho-Balkan Geological Association, XII Congress, Guidebook 18, Excursion A. 3, Bucharest*.
- CIULAVU, M. 2001. *Alpine metamorphism of danubian and severin nappe system and related ore mineral deposits*. Unpublished Ph.D. thesis. Bucharest University.
- CIULAVU, M. & SEGHEDI, A. 1997. Very low-grade Alpine metamorphism in the Danubian Window (South Carpathians, Romania). In: GRUBIC, A. & BERZA, T. (eds) *Geology of the Djerdap Area*. Geoinstitut, Belgrade, Special edition, 291–295.
- CODARCEA, A. 1940. Vues nouvelles sur la tectonique du Banat meridional et du plateau de Mehedinti. *Anuarul Geologic Institutul Al României*, **XX**, 1–74.
- CODARCEA, A. & RAILEANU, G. 1960. Mezozoicul din Carpații Meridionali. *Studii si cercetari de Geologie, Geolizică, Geografie, seria Geologie*, **4**.
- DALLA TORRE, M., DE CAPITANI, C., FREY, M., UNDERWOOD, M. B., MULLIS, J. & COX, R. 1996. Very low-temperature metamorphism of shales from the Diablo Range, Franciscan Complex, California; new constraints on the exhumation path. *Geological Society of America Bulletin*, **108**, 578–601.
- DALLA TORRE, M., FERREIRO MAEHLMANN, R. & ERNST, W. G. 1997. Experimental study on the pressure dependence of vitrinite maturation. *Geochimica et Cosmochimica Acta*, **61**, 2921–2928.
- DALLMEYER, R. D., NEUBAUER, F., HANDLER, R., FRITZ, H., PANA, D., PUTIS, M. & ANON. 1996. Tectonothermal evolution of the internal Alps and Carpathians; evidence from <sup>40</sup>Ar/<sup>39</sup>Ar mineral and whole-rock data; *International Geological Congress, Abstracts—Congres Geologique International, Resumes*, **1**, 180.
- DE CARITAT, P., HUTCHEON, I. & WALSHE, J. L. 1993. Chlorite geothermometry; a review. *Clays and Clay Minerals*, **41**, 219–239.
- DUNKL, I., GRASEMANN, B. & FRISCH, W. 1998. Thermal effects of exhumation of a metamorphic core complex on hanging wall syn-rift sediments: an example from the Rechnitz window, eastern Alps. *Tectonophysics*, **297**, 31–50.
- ELLIOT, W. C., EDENFIELD, N. M., WAMPLER, J. M., MATISOFF, G. & LONG, P. E. 1999. The kinetics of the smectite to illite transformation in Cretaceous bentonites, Cerro Negro, New Mexico. *Clays and Clay Minerals*, **47**, 286–296.
- ERNST, W. G. & FERREIRO MÄHLMANN, R. 2004. Vitrinite alteration rate as a function of temperature, time, starting material, aqueous fluid pressure, and oxygen fugacity—Laboratory corroboration of prior work. In: HILL, R. J., LEVENTHAL, J., AIZENSHTAT, M. J. ET AL. (eds) *Geochemical Investigations in Earth and Space Sciences: A Tribute to Isaac R. Kaplan*. The Geochemical Society, 341–357.
- FERREIRO MÄHLMANN, R. 1994. *Zur Bestimmung von Diagenesehöhe und beginnender Metamorphose—Temperaturgeschichte und Tektogenese des Austroalpins und Südpenninikums in Voralberg und Mittelbünden* [Published Ph.D. thesis]. *Frankfurter Geowissenschaftliche Arbeiten, Serie C*, **14**, 1–498.
- FERREIRO MÄHLMANN, R. 1995. The pattern of diagenesis and metamorphism by vitrinite reflectance and illite-crystallinity in Mittelbünden and in the Oberhalbstein. 1. The relationship to stockwerk tectonics. *Schweizerische Mineralogische und Petrographische Mitteilungen*, **75**, 85–122.
- FERREIRO MÄHLMANN, R. 1996. The pattern of diagenesis and metamorphism by vitrinite reflectance and illite 'crystallinity' in Mittelbünden and in the Oberhalbstein. 2. Correlation of coal petrography and of mineralogical parameters. *Schweizerische Mineralogische und Petrographische Mitteilungen*, **76**, 23–46.
- FERREIRO MÄHLMANN, R. 2001. Correlation of very low grade data to calibrate a thermal maturity model in a

- nappe tectonic setting, a case study from the Alps. *Tectonophysics*, **334**, 1–33.
- FERREIRO MÄHLMANN, R., BELMAR, M. & CIULAVU, M. 2001. Bituminite reflectance in very low grade metamorphic studies. Key Note Lecture, Terra Abstracts. *Journal of Conference Abstracts*, EUG 11, **6/1**, 230.
- FERREIRO MÄHLMANN, R., PETROVA, T. V., PIRONON, J., STERN, W. B., GHANBAJA, J., DUBESSY, J. & FREY, M. 2002. Transmission electron microscopy study of carbonaceous material in a metamorphic profile from diagenesis to amphibolite facies (Bündnerschiefer, Eastern Switzerland). *Schweizerische Mineralogische und Petrographische Mitteilungen*, **82**, 253–272.
- FREY, M. 1968. Zur Metamorphose des Keupers vom Tafeljura bis zum Lukmanier-Gebiet. *Schweizerische Mineralogische und Petrographische Mitteilungen*, **48**, 829–831.
- FREY, M. 1969. A mixed layer paragonite/phengite of low-grade metamorphic origin. *Contributions in Mineralogy and Petrology*, **24**, 63–65.
- FREY, M. 1978. Progressive low-grade metamorphism of a black shale formation, central Swiss Alps, with special reference to pyrophyllite and margarite bearing assemblages. *Journal of Petrology*, **19**, 95–135.
- FREY, M. 1986. Very low-grade metamorphism of the Alps: an introduction. *Schweizerische Mineralogische und Petrographische Mitteilungen*, **66**, 13–27.
- FREY, M. 1987a. The reaction-isograd kaolinite + quartz = pyrophyllite + H<sub>2</sub>O, Helvetic Alps, Switzerland. *Schweizerische Mineralogische und Petrographische Mitteilungen*, **67**, 1–11.
- FREY, M. 1987b. Very low-grade metamorphism of clastic sedimentary rocks. In: FREY, M. (ed.) *Low Temperature Metamorphism*. Blackie and Son Ltd., Glasgow and London, 9–58.
- FREY, M., DE CAPITANI, C. & LIOU, J. G. 1991. A new petrogenetic grid for low-grade metabasites. *Journal of Metamorphic Geology*, **9**, 497–509.
- FREY, M., DESMONS, J. & NEUBAUER, F. 1999. Alpine Metamorphic Map 1:50 000; Pre-Alpine Metamorphic Map 1:1000 000. In: FREY, M., DESMONS, J. & NEUBAUER, F. (eds) *The new metamorphic map of the Alps*. *Schweizerische Mineralogische und Petrographische Mitteilungen*, **79**, 1–4.
- FREY, M. & FERREIRO MÄHLMANN, R. 1999. Alpine metamorphism of the Central Alps. *Schweizerische Mineralogische und Petrographische Mitteilungen*, **79**, 135–154.
- FREY, M. & ROBINSON, D. 1999. *Low-Grade Metamorphism*. Oxford, Blackwell Sciences.
- FREY, M., TEICHMUELLER, M., TEICHMUELLER, R. ET AL. 1980. Very low-grade metamorphism in external parts of the Central Alps; illite crystallinity, coal rank and fluid inclusion data. *Eclogae Geologicae Helveticae*, **73**, 173–203.
- FREY, M. & WIELAND, B. 1975. Chloritoid in autochthon-parautochthonen Sedimenten des Aarmassivs. *Schweizerische Mineralogische und Petrographische Mitteilungen*, **55**, 407–418.
- FÜGENSCHUH, B. & SCHMID, S. M. 2005. Age and significance of core complex formation in a very curved orogen: Evidence from fission track studies in the South Carpathians (Romania). *Tectonophysics*, **404**, 33–53.
- FÜGENSCHUH, B., SEWARD, D. & MANCKTELOW, N. 1997. Exhumation in a convergent orogen: the western Tauern window. *Terra Nova*, **9**, 213–217.
- GENSER, J., VAN WEES, J. D., CLOETINGH, S. & NEUBAUER, F. 1996. Eastern Alpine tectono-metamorphic evolution: Constraints from two-dimensional P–T–t modeling. *Tectonics*, **15**, 584–604.
- GHENT, E. D., STOUT, M. Z. & FERRI, F. 1989. Chloritoid, paragonite, pyrophyllite and stilpnomelane-bearing rocks near Blackwater Mountain, Western Rocky Mountains, British Columbia. *Canadian Mineralogist*, **27**, 59–66.
- GRUNENFELDER, M., POPESCU, G., SOROIU, M., ARSENESCU, V. & BERZA, T. 1983. K–Ar and U–Pb dating of the metamorphic formations and the associated igneous bodies of the Central South Carpathians. *Anuarul Geologic Institutul Al României*, **61**, 37–46.
- HEMLEY, J. J., MONTOYA, J. W., MARINENKO, J. W. & LUCE, R. W. 1980. Equilibria in the system Al<sub>2</sub>O<sub>3</sub>–SiO<sub>2</sub>–H<sub>2</sub>O and some general implications for alteration/mineralization processes. *Economic Geology and the Bulletin of the Society of Economic Geologists*, **75**, 210–228.
- HOOD, A., GUTJAHR, C. C. M. & HEACOCK, R. L. 1975. Organic metamorphism and the generation of petroleum. *American Association of Petroleum Geologists Bulletin*, **59**, 986–996.
- HUNT, J. M., LEWAN, M. D. & HENNET, R. J. C. 1991. Modeling oil generation with Time-Temperature Index graphs based on the Arrhenius Equation. *American Association of Petroleum Geologists Bulletin*, **75**, 795–807.
- IANCU, V. 1986. Mineral assemblages in low grade metamorphic rocks in the South Carpathians; Mineral parageneses. *Theophrastus Publications S. A., Athens*, 503–519.
- IANCU, V. & MARUNTIU, M. 1994. Pre-Alpine litho-tectonic units and related shear zones in the basement of the Getic-Supragetic nappes (South Carpathians). *Romanian Journal of Tectonics and Regional Geology (Suppl. 2: ALCAPA II Field Guidebook)*, **75**, 87–92.
- IANCU, V., UDUBASA, G., RADAN, S., VISARION, A. & ANON. 1984. Complex criteria of separating weakly metamorphosed formations; an example, the South Carpathians; Volume special; Congres geologic international. *Anuarul Institutului de Geologie si Geofizica*, **64**, 51–60.
- IANOVICI, V., NEACSU, G., NEACSU, V. ET AL. 1981. Pyrophyllite occurrences and their genetic relations with the kaolin minerals in Romania. *26eme Congres geologique international: Symposium interactions fluides, mineraux, roches. Bulletin de Mineralogie*, **104**, 768–775.
- JACOB, H. 1989. Classification, structure, genesis and practical importance of natural solid oil bitumen (Migrabitumen). *International Journal of Coal Geology*, **11**, 65–79.
- JACOB, H. & HILTMANN, W. 1985. Disperse, feste Erdöl-bitumina als Migrations- und Maturitätsindikatoren im Rahmen der Erdöl- und Erdgas-Prospektion. Eine Modellstudie in Nordwestdeutschland. *Deutsche Wissenschaftliche Gesellschaft für Erdöl, Erdgas und Kohle, Forschungsberichte*, **267**, 1–54.

- JIANG, W. T., PEACOR, D. R. & BUSECK, P. R. 1994. Chlorite Geothermometry—Contamination and Apparent Octahedral Vacancies. *Clays and Clay Minerals*, **42**, 593–605.
- KISCH, H. J. 1987. Correlation between indicators of very low-grade metamorphism. In: FREY, M. (ed.) *Low Temperature Metamorphism*. Blackie and Son Ltd., Glasgow and London, 227–300.
- KOCH, J. 1997. Organic petrographic investigations of the Kupferschiefer in northern Germany. *International Journal of Coal Geology*, **33**, 301–316.
- KOONS, P. O. 1987. Some thermal and mechanical consequences of rapid uplift; an example from the Southern Alps, New Zealand. *Earth and Planetary Science Letters*, **86**, 307–319.
- KRUMM, H., PETSCHICK, R. & WOLF, M. 1988. From diagenesis to anchimetamorphism, Upper Austroalpine sedimentary cover in Bavaria and Tyrol. *Geodinamica Acta*, **2**, 33–47.
- KRETZ, R. 1983. Symbol for rock-forming minerals. *American Mineralogist*, **68**, 277–279.
- KÜBLER, B. 1967. *La cristallinité de l'illite et les zones tout à fait supérieures du métamorphisme. Etage tectoniques*. Colloquium Neuchâtel, 18–21 avril 1967, 105–122.
- LEMNE, M., SAVU, H., STEFAN, A., BORCOS, M., SÂNDULESCU, D., UDUBASA, G., VAIDEA, E., ROMANESQUE, O., TANASESCU, A. & IOSIPENCO, N. 1983. *Date geocronologie privind formatiuni metamifice si magmatice din Romania*. Report Arhiva Geologic Institutul al României, Bucuresti.
- LIVI, K. J. T., VEULEN, D. R., FERRY, J. M. & FREY, M. 1997. Evolution of 2:1 layered silicates in low-grade metamorphosed Liassic shales of Central Switzerland. *Journal of Metamorphic Geology*, **15**, 323–344.
- MANCKTELOW, N. S. & GRASEMANN, B. 1997. Time-dependent effects of heat advection and topography on cooling histories during erosion. *Tectonophysics*, **270**, 167–195.
- MANOLESCU, G. 1937. Etude géologique et pétrographique dans les Muntii Vulcan (Carpatés méridionales, Roumanie). *Anuarul Geologic Institutul Al României*, **XVIII**, 79–172.
- MARUNTIU, M. 1987. *Studiul geologic complex al rocilor ultrabazice din Carpatii Meridionali*. [unpublished Ph.D. thesis], Bucharest University.
- MARUYAMA, S., CHO, M. & LIU, J. G. 1986. Experimental investigations of blueschist-greenschist transition equilibria; pressure dependence of Al<sub>2</sub>O<sub>3</sub> contents in sodic amphiboles; a new geobarometer; Blueschists and eclogites. *Memoir Geological Society of America*, **164**, 1–16.
- MASSONNE, H. J. & SCHREYER, W. 1987. Phengite geobarometry based on the limiting assemblage with K-feldspar, phlogopite, and quartz. *Contributions to Mineralogy and Petrology*, **96**, 212–224.
- MATENCO, L., BERTOTTI, G., DINU, C. & CLOETINGH, S. 1997. Tertiary tectonic evolution of the external South Carpathians and the adjacent Moesian platform (Romania). *Tectonics*, **16**, 896–911.
- MATENCO, L. & SCHMID, S. 1999. Exhumation of the Danubian nappes system (South Carpathians) during the Early Tertiary: inferences from kinematic and paleostress analysis at the Getic/Danubian nappes contact. *Tectonophysics*, **314**, 401–422.
- MERRIMAN, R. J. & FREY, M. 1999. Patterns of very low-grade metamorphism in metapelitic rocks. In: FREY, M. & ROBINSON, D. (eds) *Low-Grade Metamorphism*. Blackwell Sciences, Oxford, 61–107.
- MRAZEC, L. 1898. *Dare de sema asupra cercetarilor geologice din vara 1897. I: Partea de E a muntilor Vulcan*. *Buletinul Ministerului Agriculturii si Domeniilor*, 39p.
- MURGOCI, G. M. 1905. *Sur l'existence d'une grande nappe de recouvrement dans les Carpathes Méridionales*. Unpublished thesis, Comptes Rendus de l'Académie des Sciences, Paris.
- MURGOCI, G. M. 1912. The geological synthesis of the South Carpathians. *Compte Rendu du XI-eme Congres Geologique International*, 871–881.
- NĂSTĂSEANU, S. V. 1979. *Geologie des Monts Cerna*. *Anuarul Institutului de Geologie si Geofizica*, **54**, 153–280.
- NĂSTĂSEANU, S. V., RUSSO-SANDULESCU, D., BERDIA, I., SAVU, H., MARUNTEANU, M., RUSU, A. & BERDIA, E. 1985. *Geological Map of Romania, scale 1:50 000, sheet Comereva*. Geologic Institutul al României, Bucuresti.
- PALIUC, G. 1972. *Pirofilitul din formatiunea de Schela*. *Dari de Seama Ale Sedintelor, Comitetul de Stat al Geologiei*, **58**, 45–65.
- PETROVA, T. V., FERREIRO MÄHLMANN, R., STERN, W. B. & FREY, M. 2002. Application of combustion and DTA-TGA analysis to the study of metamorphic organic matter. *Schweizerische Mineralogische und Petrographische Mitteilungen*, **82**, 33–53.
- POP, G. 1973. *Depozitele mezozoice din Muntii Vulcan*. *Editura Academiei, Bucuresti*.
- POPCU, G. C., TATU, M. & DAMIAN, G. 1982. La reflectivité et les caractéristiques oroentogéologiques de l'Anthracite de la formation de Schela. *Analele Universitatii Bucuresti, Geologie*, **31**, 13–20.
- POTEL, S., FERREIRO MÄHLMANN, R., STERN, W. B., MULLIS, J. & FREY, M. 2006. Very low-grade metamorphic evolution of pelitic rocks under high-pressure/low-temperature conditions, NW New Caledonia (SW Pacific). *Journal of Petrology*, **47**, 991–1015.
- POTEL, S., SCHMIDT, S. T. & DE CAPITANI, C. 2002. Composition of pumpellyite, epidote and chlorite from New Caledonia — How important are metamorphic grade and whole-rock composition? *Schweizerische Mineralogische und Petrographische Mitteilungen*, **82**, 229–252.
- RADTKE, M., SCHAEFFER, R. G., LEITHAUSER, D. & TEICHMÜLLER, M. 1980. Composition of soluble organic matter in coals: relation to rank and liptinite fluorescence. *Geochimica Cosmochimica Acta*, **44**, 1787–1800.
- RAHN, M., MULLIS, J., ERDELBROCK, K. & FREY, M. 1994. Very low-grade metamorphism of the Taveyanne Greywacke, Glarus Alps, Switzerland. *Journal of Metamorphic Geology*, **12**, 625–641.
- RAMDOHR, P. 1928. *Mikroskopische Beobachtungen an Graphiten und Koksen*. *Archiv für Eisenhüttenwesen*, **1**, 669–672.
- RATSCHBACHER, L., LINZER, H. G., MOSER, F., STRUSIEVICZ, R. O., BEDELEAN, H., HAR, N. &

- MOGOS, P. A. 1993. Cretaceous to Miocene thrusting and wrenching along the Central South Carpathians due to a corner effect during collision and orocline formation. *Tectonics*, **12**, 855–873.
- ROBERT, P. 1988. Organic metamorphism and geothermal history—Microscopic study of organic matter and thermal evolution of sedimentary basins. *Elf-Aquitaine and D. Reidel Publishing Company*, Nordrecht.
- ROBINSON, D. & BEVINS, R. E. 1999. Patterns of regional low-grade metamorphism in metabasites. In: FREY, M. & ROBINSON, D. (eds) *Low-Grade Metamorphism*. Blackwell Sciences, 143–168.
- SACHSENHOFER, R. F. 2001. Syn- and post-collisional heat flow in the Cenozoic Eastern Alps. *International Journal of Earth Sciences*, **90**, 579–592.
- SÂNDULESCU, M. 1975. Essai de synthese structurale des Carpathes. *Bulletin de la Societe Geologique de France*, **17**, 299–358.
- SÂNDULESCU, M. 1984. Geotectonica Romaniei. *Editura Tehnica*, Bucharest, 334p.
- SÂNDULESCU, M. 1994. Overview of Romanian geology. Abstracts volume ALCAPA II Symposium, Covasna 1994. *Romanian Journal of Tectonics and Regional Geology*, **75**, supplement number 2, 57.
- SAVU, H. 1970. Structura plutonului Susita si relatiile sale cu formatiunile autohtonului danubian (Carpatii meridionali). *Dari de Seama ale Institutului Geologic*, **LVI/5**, 123–153.
- SAVU, H., UDRESCU, C., NEACSU, V., BRATOSIN, I. & STOIAN, M. 1985. Origin, geochemistry and tectonic position of the Alpine ophiolites in the Severin Nappe (Mahedinti Plateau, Romania); Ophiolites through time; proceedings. *Ophioliti*, **10**, 423–440.
- SCHMID, S. M., BERZA, T., DIACONESCU, V., FROITZHEIM, N. & FÜGENSCHUH, B. 1998. Orogen-parallel extension in the Southern Carpathians. *Tectonophysics*, **297**, 209–228.
- SCHMIDT, D., SCHMIDT, S. T., MULLIS, J., FERREIRO MÁHLMANN, R. & FREY, M. 1997. Very low grade metamorphism of the Taveyane formation of western Switzerland. *Contributions to Mineralogy and Petrology*, **129**, 385–403.
- SEGHEDI, A. & BERZA, T. 1994. Duplex interpretation for the structure of the Danubian Thrust Sheets. Abstracts volume ALCAPA II Symposium, Covasna 1994. *Romanian Journal of Tectonics and Regional Geology*, **75**(1), 57.
- SEKI, Y. 1972. Lower-grade stability limit of epidote in the light of natural occurrences. *Journal of the Geological Society of Japan*, **78/8**, 405–413.
- SPERLICH, R. 1988. The transition from crossite to actinolite in metabasites of the Combin unit in Valle St. Barthelemy (Aosta, Italy). *Schweizerische Mineralogische und Petrographische Mitteilungen—Bulletin Suisse de Mineralogie et Petrographie*, **68**, 215–224.
- STACH, F., MACKOWSKY, M. T., TEICHMÜLLER, M., TAYLOR, G. H., CHANDRA, D. & TEICHMÜLLER, R. 1982. *Textbook of Coal Petrology*, Borträger, Stuttgart.
- STĂNOIU, I. 1972. Incercare de reconstituire a succesiunii Paleozoicului din partea de est a autohtonului danubian, cu privire speciala asupra regiunii de la obisia vaii Motru (Carpatii Meridionali). *Dari de Seama ale Institutului Geologic*, **LVIII/4**, 57–71.
- STĂNOIU, I. 1973. Zona Mehedinti-Retezat, o unitate paleogeografica si tectonica distincta a Carpatilor Meridionali. *Dari de Seama ale Institutului Geologic*, **59/5**, 127–171.
- STĂNOIU, I., UDUBASA, G., RADAN, S. & VANGHELIE, I. 1982. Cercetarea complexa a formatiunilor purtatoare de carbuni si sisturi combustibile din Carpatii Meridionali—Versantul nordic al masivului Vilcan. Conturarea domeniului de extindere a formatiunii liasice purtatoare de antracit din versantul nordic al masivului Vilcan. *Arhiva Geologic Institutul Al Romaniei, Bucuresti*.
- STĂNOIU, I., CONOVICI, M., MARINESCU, F., RUSSO-SÂNDULESCU, D., AERBĂNESCU, A. & VANGHELIE, I. 1988. Harta geologica a Romaniei, scara 1 : 50000, foaia Balta: Arh. IGG.
- SUCHY, V., FREY, M. & WOLF, M. 1997. Vitrinite reflectance and shear-induced graphitization in orogenic belts: a case study from the Kandersteg area, Helvetic Alps, Switzerland. *International Journal of Coal Geology*, **34**, 1–20.
- TEICHMÜLLER, M. 1987. Organic material and very low-grade metamorphism. In: FREY, M. (ed.) *Low Temperature Metamorphism*. Blackie and Son Ltd., Glasgow and London, 114–160.
- THEYE, T. 1988. *Aufsteigende Hochdruckmetamorphose in Sedimenten der Phyllit-Quarzit-Einheit Kretas und des Peloponnes*. Unpublished Ph.D. thesis, Technische Universität, Braunschweig.
- THEYE, T., SCHREYER, W. & FRANSOLET, A. M. 1996. Low-temperature, low-pressure metamorphism of Mn-rich rocks in the Lienne syncline, Venn-Stavelot Massif (Belgian Ardennes), and the role of carpholite. *Journal of Petrology*, **37**, 767–783.
- THEYE, T. & SEIDEL, E. 1991. Petrology of low-grade high-pressure metapelites from the external Hellenides (Crete, Peloponnese)—a case-study with attention to sodic minerals. *European Journal of Mineralogy*, **3**, 343–366.
- THOMPSON, A. B. 1970. A note on the kaolinite-pyrophyllite equilibrium. *American Journal of Science*, **268**, 454–458.
- VIDAL, O., GOFFÉ, B., BOUSQUET, R. & PARRA, T. 1999. Calibration and testing of an empirical chloritoid-chlorite Mg–Fe exchange thermometer and thermodynamic data for daphnite. *Journal of Metamorphic Geology*, **17**, 25–39.
- WAPLES, D. W. 1980. Time and temperature in petroleum formation; application of Lopatin's method to petroleum exploration. *American Association of Petroleum Geologists Bulletin*, **64**, 916–926.
- WILLINGSHOFER, E. 2000. Extension in collisional orogenic belts: the Late Cretaceous evolution of the Alps and Carpathians. Unpublished Ph.D. thesis, Vrije Universiteit Amsterdam, Amsterdam.
- WOLF, M. 1975. Über die Beziehungen zwischen Illit-Kristallinität und Inkohlung. *Neues Jahrbuch für Geologie und Paläontologie*, 437–447.
- WOLF, M. & WOLFF-FISCHER, E. 1984. Alginite in Humuskohlen karbonischen Alters und sein Einfluss auf die optischen Eigenschaften des begleitenden Vitrinites. *Glückauf Forschungshefte*, **45**, 243–246.
- ZEN, E. A. 1960. Metamorphism of lower Paleozoic rocks in the vicinity of the Taconic Range in west-central Vermont. *American Mineralogist*, **45**, 129–175.